

655

for Aeronautics

MAILED

JAN 31 1936

To: *Library L. M. A. L.*

TECHNICAL NOTES

NATIONAL ADVISORY COMMITTEE FOR AERONAUTICS

No. 551

TANK TESTS OF THREE MODELS OF FLYING-BOAT HULLS
OF THE POINTED-STEP TYPE WITH DIFFERENT ANGLES
OF DEAD RISE - N.A.C.A. MODEL 35 SERIES

By John R. Dawson
Langley Memorial Aeronautical Laboratory

Washington
January 1936

NATIONAL ADVISORY COMMITTEE FOR AERONAUTICS

TECHNICAL NOTE NO. 551

TANK TESTS OF THREE MODELS OF FLYING-BOAT HULLS
OF THE POINTED-STEP TYPE WITH DIFFERENT ANGLES
OF DEAD RISE - N.A.C.A. MODEL 35 SERIES

By John R. Dawson

SUMMARY

The results of tank tests of three models of flying-boat hulls of the pointed-step type with different angles of dead rise are given in charts and are compared with results from tests of more conventional hulls. Increasing the angle of dead rise from 15° to 25° : had little effect on the hump resistance; increased the resistance throughout the planing range; increased the best trim angle; reduced the maximum positive trimming moment required to obtain best trim angle; and had but a slight effect on the spray characteristics. For approximately the same angles of dead rise the resistances of the pointed-step hulls were considerably lower at high speeds than those of the more conventional hulls.

INTRODUCTION

N.A.C.A. model 35 is a pointed-step flying-boat hull of high length-beam ratio designed particularly to give low resistance at high speeds. Tank tests of this model have been reported in reference 1. It was believed that by making landings on the point of the step a low angle of dead rise could be used with the pointed-step type of hull. There has, however, been considerable criticism of the low angles of dead rise incorporated in the pointed-step models that have been tested at the tank. One criticism was that, in view of the large bottom pressures that have been found in delayed take-offs of seaplanes with higher angles of dead rise, the low angles of dead rise of these models would probably result in excessive bottom pressures during take-off.

Tests of planing surfaces made at the N.A.C.A. tank (reference 2) show that increasing the angle of dead rise increases the resistance in the planing range, but these data are strictly applicable to a flying-boat hull only when the form of the bottom of the forebody is similar to the planing surfaces tested and when the afterbody is completely clear of the water. The afterbody of model 35 is clear of the water when planing at best trim angle, but the forebody ends with a step that is pointed in plan form whereas the sterns of the planing surfaces were cut off square.

Because it was believed that even with a high angle of dead rise the pointed-step-type hull would have relatively low resistance at high speeds, tank tests were made of two additional models with higher angles of dead rise.

THE MODELS

Three different models were used in the tests, model 35 (15° angle of dead rise), model 35-A (20°), and model 35-B (25°). Model 35 is the same model that was used in the test reported in reference 1. Models 35-A and 35-B were derived from model 35 by increasing the angle of dead rise of that portion of the hull of which the angle of dead rise is constant and by raising all points on the buttock lines in proportion to their heights above the straight portion of the forebody keel. The only other change resulting from the change of angle of dead rise is the raising of the bow, which is necessary to compensate for the higher chines caused by the increased angle of dead rise. The tail appendage, which is usually added to a hull for the purpose of carrying the tail surfaces of the airplane, was left off for simplicity. The plan form is the same for each model (fig. 1); the offsets are given in tables I to III.

In accordance with the usual practice at the N.A.C.A. tank, the models were made of laminated wood, sanded, painted, and rubbed to give a smooth surface.

APPARATUS AND PROCEDURE

The N.A.C.A. tank, its carriage, and some of the

testing apparatus are described in reference 3. The towing gear used is generally similar to that described in reference 2, but has a very stiff spring for measuring trimming moments. The deflections of this spring are measured on a dial gage and are so small that the trim angle remains fixed within the accuracy to which it may be determined. The towing gear was restrained from lateral movement by guide wheels attached to the gear and allowed to roll on a vertical staff rigidly attached to the carriage.

The test program followed the general method, in which the model is towed at a succession of fixed trim angles with a number of constant loads, and a sufficient number of trim angles are used to determine the trim angle that gives minimum resistance (called "best trim angle"). The models were tested over an unusually wide range of loads and speeds because they are suitable for seaplane floats as well as for flying-boat hulls.

Although model 35 had been tested previously, the test was repeated to insure identical testing conditions for the three models. More points were obtained in the present tests than in the original test of model 35. The increased capacity of the moment-measuring gear eliminated extrapolation, which was necessary in some cases with the original tests.

RESULTS

Test Data

Resistance (including the air drag of the model), trimming moment, and draft are plotted against speed with load as parameter in figures 2 to 19. Each figure shows the data for one trim angle. The center of moments used in the tests is shown in figure 1; moments tending to raise the bow are considered positive. All drafts are measured at the after end of the step as it is a convenient point of reference although at high trim angles the sternpost is deeper in the water.

Static drafts and trimming moments for models 35-A and 35-B are given in figures 20 and 21, in which trimming moment is plotted against trim angle with displacement as parameter, and drafts are plotted against dis-

placement with trim angle as parameter. These data may be used in the determination of load water lines on the hulls at rest. No static curves are given for model 35 because they are already available in reference 1.

Nondimensional Data

In order to eliminate the trim-angle variable, the trim angle that gives minimum resistance is determined by cross-plotting resistance against trim angle with load and speed as parameters. Speed, load, minimum resistance, and the trimming moment to obtain minimum resistance are converted to the following nondimensional coefficients:

$$\text{Speed coefficient, } C_V = \frac{V}{\sqrt{gb}}$$

$$\text{Load coefficient, } C_\Delta = \frac{\Delta}{wb^3}$$

$$\text{Resistance coefficient, } C_R = \frac{R}{wb^3}$$

$$\text{Trimming-moment coefficient, } C_M = \frac{M}{wb^4}$$

where

V is speed, ft./sec.

g , acceleration of gravity, ft./sec.²

b , maximum beam of hull, ft.

Δ , load on water, lb.

w , specific weight of water, lb./cu.ft. ($w = 63.5$ lb./cu.ft. for the water in the N.A.C.A. tank during these tests).

R , resistance, lb.

M , trimming moment, lb.-ft.

Any other consistent set of units may, of course, be used.

The data for best trim angle converted to these coefficients are plotted in figures 22 to 33 for all three models. In figures 22 to 24 the minimum value of C_R is plotted against C_V with C_Δ as parameter; in figures 25 to 27 the minimum value of C_R is plotted against C_Δ with C_V as parameter. The curves of figures 25 to 27 are more useful in making take-off calculations than those of figures 22 to 24 because C_R for any value of C_Δ can be read directly. In figures 28 to 30, the best trim angle τ_0 is plotted against C_V with C_Δ as parameter; in figures 31 to 33 the trimming-moment coefficient C_M required to obtain τ_0 is plotted against C_V with C_Δ as parameter.

Neither τ_0 nor C_M is shown for values of C_Δ greater than 1.2 because the curves of resistance against trim angle for the 120-pound load did not consistently show a minimum for any of the models tested. In the low-speed range where this condition occurs the best trim angle is relatively unimportant because the resistance does not vary greatly with trim angle at those speeds. For load coefficients greater than 1.2 the plotted values of C_R correspond to the least resistance obtained in the tests whether they were shown to be minimums or not. In take-off calculations, the τ_0 for values of C_Δ greater than 1.2 may be assumed to be about the same as τ_0 for $C_\Delta = 1.2$. The resistance at any trim angle may, of course, be determined by cross-plotting the curves of test data.

DISCUSSION OF RESULTS

The present data for model 35 check reasonably well with the data from the original test published in reference 1. The resistance curve, however, comes to a rather critical peak at the hump and some large discrepancies are found at the heaviest loads in this region; the hump is somewhat better defined in the present tests by a closer spacing of test points. The large discrepancies found in the maximum positive trimming-moment coefficient and the maximum best trim angle are caused by extrapolation of data in the original tests.

In figure 34 a comparison is made of the resistance coefficients at best trim angle for the three models tested. In this figure C_R for all three models is plotted against C_v at several values of C_Δ . The differences in the resistance at the hump are small considering the difficulty of obtaining the absolute maximum where the hump is critical. In the planing region, however, there is a well-defined increase in resistance with increased angle of dead rise, the same trend that was observed in the tests of planing surfaces. At values of C_v greater than about 4 the afterbodies of these models are completely clear of the water when the models are running at best trim angle so that the models may be considered as single, pointed-stern planing surfaces throughout the high-speed range.

Figures 28 to 30 show that the best trim angle throughout the planing range is increased as the angle of dead rise is increased. Maximum positive values of C_M at best trim angle are plotted in figure 35 for the three models. Increase in angle of dead rise caused a decrease in maximum positive C_M for all loads, due in part to the increased best trim angle. The maximum moments all occur at a somewhat higher speed than that at which the resistance hump occurs.

At the hump speeds the spray from all three models was nearly the same. At higher speeds, an increased angle of dead rise caused a slight increase in the angle at which the spray was thrown upward.

In reference 1 some directional instability was noted for model 35 at low speeds. Inasmuch as the towing-gear arrangement used in the present tests prevented the models from showing this tendency, the restraining rollers on the gear were later removed and models 35-A and 35-B were run at constant speed throughout the range in which the directional instability is likely to occur. Although some directional instability was noted on models 35-A and 35-B, the range of speeds in which it occurred appeared to be shorter than for model 35.

A comparison of the resistance of models 35-A and 35-B with the resistance of more conventional forms having corresponding angles of dead rise should show the relative value of the pointed-step-type hull.

In figure 36 models 35-A and 40-AC are compared by plotting C_R against C_V for several values of C_Δ . The angle of dead rise for both hulls is 20° . Model 40-AC (reference 4) is one of a series designed for small flying boats and amphibians and has a high length-beam ratio (5.47 excluding the tail appendage). It has a conventional main step and the afterbody is pointed in plan form similar to many existing American hulls.

The hump resistance of model 35-A is less than that of model 40-AC at the light loads and greater at the heavy loads but it occurs at a lower speed so that more thrust would be available at the hump for model 35-A. Just after the hump the resistance of model 40-AC decreases rapidly until it is below that of model 35-A except at the very light loads. As the speed is increased further the resistance of model 40-AC increases more rapidly than the resistance of model 35-A so that at high speeds the pointed-step hull is considerably better.

In figure 37 models 35-B and 11-C are compared by plotting C_R against C_V for the high-speed range. The angle of dead rise for model 11-C is $22\text{-}1/2^\circ$ and for model 35-B it is 25° . Model 11-C (reference 5) is similar in type to model 40-AC but its length-beam ratio is considerably smaller. In a comparison of models of widely different length-beam ratios the effect of length-beam ratio generally tends to obscure other effects. At high speeds, however, the afterbody of the pointed-step hull is clear when running at best trim angle and a large portion of the forebody is out of the water and therefore not effective. Under these conditions changes in the length of the hull have a negligible effect on the water resistance and the comparison shown in figure 37 is hardly affected by the large difference in the length-beam ratios of the two models.

This second comparison shows in the high-speed range the same tendencies that were noted in figure 36. Thus it appears that the pointed-step-type hull, even with a high angle of dead rise, is particularly adapted to designs with high get-away speeds.

CONCLUSIONS

1. The tests on the model 35 series show that increas-

ing the dead rise causes the following changes in characteristics:

- (a) The resistance throughout the planing range is increased but the hump resistance is only slightly changed.
- (b) The spray characteristics are not changed greatly but at high speeds the spray is thrown up at a slightly steeper angle.
- (c) The best trim angle is increased.
- (d) The maximum positive trimming moment required to obtain best trim angle is decreased.

2. The pointed-step-type hull, even with a high angle of dead rise, appears to be especially suited for seaplanes with high get-away speeds.

Langley Memorial Aeronautical Laboratory,
National Advisory Committee for Aeronautics,
Langley Field, Va., November 15, 1935.

REFERENCES

1. Shoemaker, James M., and Bell, Joe, W.: Complete Tank Tests of Two Flying-Boat Hulls with Pointed Steps - N.A.C.A. Models 22-A and 35. T.N. No. 504, N.A.C.A., 1934.
2. Shoemaker, James M.: Tank Tests of Flat and V-Bottom Planing Surfaces. T.N. No. 509, N.A.C.A., 1934.
3. Truscott, Starr: The N.A.C.A. Tank - A High-Speed Towing Basin for Testing Models of Seaplane Floats. T.R. No. 470, N.A.C.A., 1933.
4. Parkinson, John B., and Dawson, John R.: Tank Tests of N.A.C.A. Model 40 Series of Hulls for Small Flying Boats and Amphibians. T.R. No. 543, N.A.C.A., 1935.
5. Dawson, John R.: A General Tank Test of N.A.C.A. Model 11-C Flying-Boat Hull, Including the Effect of Changing the Plan Form of the Step. T.N. No. 538, N.A.C.A., 1935.

TABLE I. Offsets for N.A.C.A. Model 35 Flying-Boat Hull (Inches)

Sta- tion	Dis- tance from F.P.	Distance from base line								Half breadths							
		Keel	¹ B1 1.30	B2 2.60	B3 3.90	B4 5.20	Main chine	Cove	Upper chine	Main chine	Cove	Upper chine	² WL1 10.00	WL2 9.00	WL3 8.00	WL4 7.00	WL5 6.00
F.P.	0.00	5.00					5.00			Tan. to F.P.							
1/2	1.25	8.35	6.48	5.65			5.60			2.86					0.26	0.85	1.87
1	2.50	9.37	7.67	6.62			6.13			3.85				0.32	1.00	2.00	
1-1/2	4.75	10.33	9.04	7.98	7.30		6.98			4.94			0.37	1.34	2.55	4.82	
2	7.00	10.76	9.82	8.93	8.24	7.77	7.68			5.58			1.04	2.49	4.49		
3	11.50	10.99	10.48	9.91	9.38	8.94	8.65			6.25			2.40	4.97			
4	16.00	11.00	Elements of stations straight lines from here aft				9.14			6.49							
5	20.50	11.00	¹ Distance from cen- ter line (plane of symmetry) to buttock (section of hull surface made by a vertical plane parallel to plane of symmetry)				9.29			6.50			² Distance from base line to water line (section of hull surface made by a horizontal plane par- allel to base line)				
6	25.00	11.00					9.29			6.50							
7	29.50	11.00					9.29	6.35	6.35	3.50	6.50	6.50					
8	34.00	11.00					9.35	6.41	6.35	6.25	6.25	6.50					
9	38.50	11.00					9.56	6.62	6.36	5.48	5.48	6.44					
10	43.00	11.00					9.90	6.96	6.41	4.20	4.20	6.25					
11	47.50	11.00					10.38	7.44	6.49	2.40	2.40	5.97					
12	52.00	11.00					11.00	8.06	6.60	.10	.10	5.54					
13	56.80	8.06							6.76			4.94					
14	61.60	8.06							6.96			4.19					
15	66.40	8.06							7.20			3.31					
16	71.20	8.06							7.47			2.30					
17	76.00	8.06							7.76			1.22					
S.P.	80.00	8.06							8.01			.30					

TABLE II. Offsets for N.A.C.A. Model 35-A Flying-Boat Hull (Inches)

		Distance from base line								Half breadths							
Sta- tion	Dis- tance from F.P.	Keel	B1 1.30	B2 2.60	B3 3.90	B4 5.20	Main chine	Cove	Upper chine	Main chine	Cove	Upper chine	WL1 10.00	WL2 9.00	WL3 8.00	WL4 7.00	WL5 6.00
F.P.	0.00	4.38					4.38			Ten. to F.P.							
1/2	1.25	8.05	5.96	5.04			4.98			2.86					0.25	0.82	1.78
1	2.50	9.16	7.25	6.06			5.51			3.85				0.29	.96	1.90	
1-1/2	4.75	10.23	8.74	7.51	6.71		6.36			4.94			0.34	1.25	2.37	4.13	
2	7.00	10.72	9.60	8.54	7.73	7.17	7.06			5.58			.95	2.25	3.95		
3	11.50	10.99	10.34	9.62	8.95	8.40	8.03			6.25			2.10	4.25			
4	16.00	11.00	Elements of stations straight lines from here aft				8.52			6.49							
5	20.50	11.00					8.67			6.50							
6	25.00	11.00					8.67			6.50							
7	29.50	11.00					8.67	5.73	5.73	6.50	6.50	6.50					
8	34.00	11.00					8.76	5.82	5.73	6.25	6.25	6.50					
9	38.50	11.00					9.04	6.10	5.75	5.48	5.48	6.44					
10	43.00	11.00					9.51	6.57	5.82	4.20	4.20	6.25					
11	47.50	11.00					10.17	7.23	5.92	2.40	2.40	5.97					
12	52.00	11.00					11.00	8.06	6.08	.10	.10	5.54					
13	56.80	8.06							6.31			4.94					
14	61.60	8.06							6.58			4.13					
15	66.40	8.06							6.89			3.31					
16	71.20	8.06							7.26			2.30					
17	76.00	8.06							7.66			1.22					
S.P.	80.00	8.06							7.99			.30					

TABLE III. Offsets for N.A.C.A. Model 35-B Flying-Boat Hull (Inches)

Sta- tion	Dis- tance from F.P.	Distance from base line								Half breadths							
		Keel	B1 1.30	B2 2.60	B3 3.90	B4 5.20	Main chine	Cove	Upper chine	Main chine	Cove	Upper chine	WL1 10.00	WL2 9.00	WL3 8.00	WL4 7.00	WL5 6.00
F.P.	0.00	3.73					3.73			Tan. to F.P.							
1/2	1.25	7.73	5.42	4.39			4.33			2.86					0.22	0.78	1.68
1	2.50	8.95	6.80	5.48			4.86			3.85				0.26	.90	1.79	3.45
1-1/2	4.75	10.12	8.42	7.03	6.13		5.71			4.94			0.30	1.15	2.20	3.75	
2	7.00	10.67	9.37	8.14	7.18	6.53	6.41			5.58			.88	2.09	3.58		
3	11.50	10.98	10.20	9.32	8.51	7.83	7.38			6.25			1.89	3.75	6.20		
4	16.00	11.00	Elements of stations straight lines from here aft				7.87			6.49							
5	20.50	11.00					8.02			6.50							
6	25.00	11.00					8.02			6.50							
7	29.50	11.00					8.02	5.08	5.08	6.50	6.50	6.50					
8	34.00	11.00					8.14	5.20	5.08	6.25	6.25	6.50					
9	38.50	11.00					8.49	5.55	5.10	5.48	5.48	6.44					
10	43.00	11.00					9.09	6.15	5.20	4.20	4.20	6.35					
11	47.50	11.00					9.93	6.99	5.32	2.40	2.40	5.97					
12	52.00	11.00					11.00	8.06	5.52	.10	.10	5.54					
		8.06															
13	56.80	8.06							5.80			4.94					
14	61.60	8.06							6.16			4.19					
15	66.40	8.06							6.56			3.31					
16	71.20	8.06							7.03			2.30					
17	76.00	8.06							7.54			1.22					
S.P.	80.00	8.06							7.97			.30					

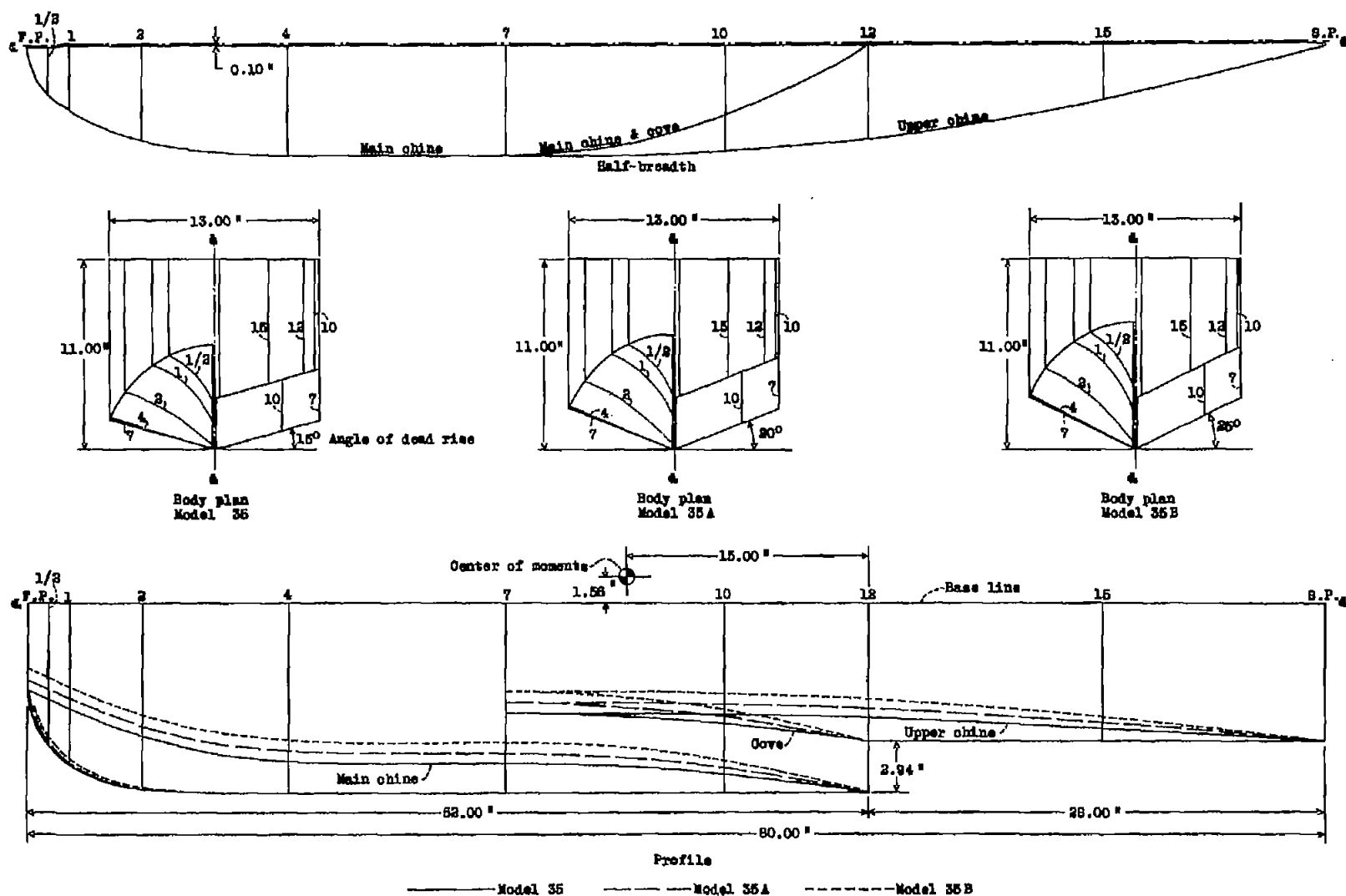
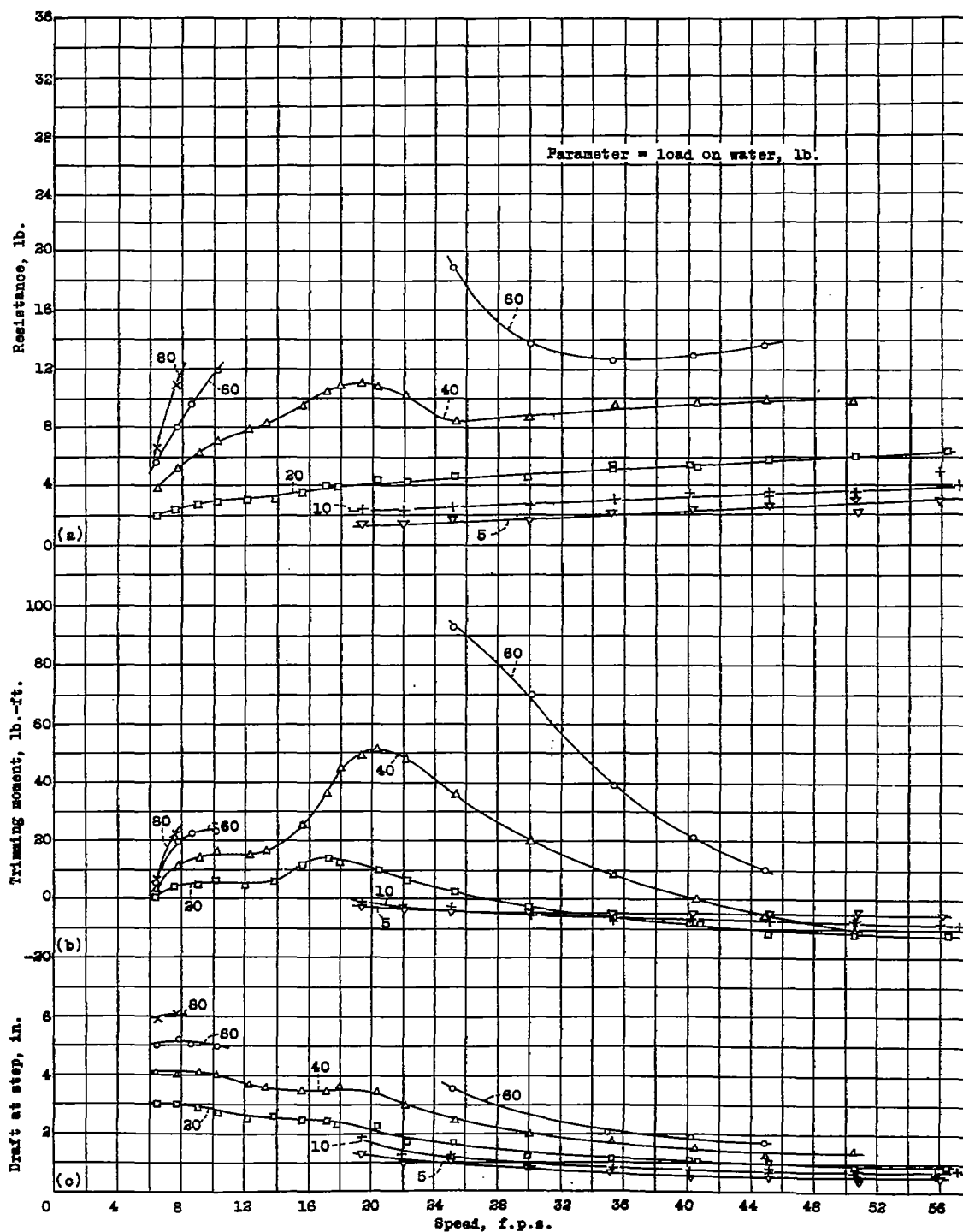
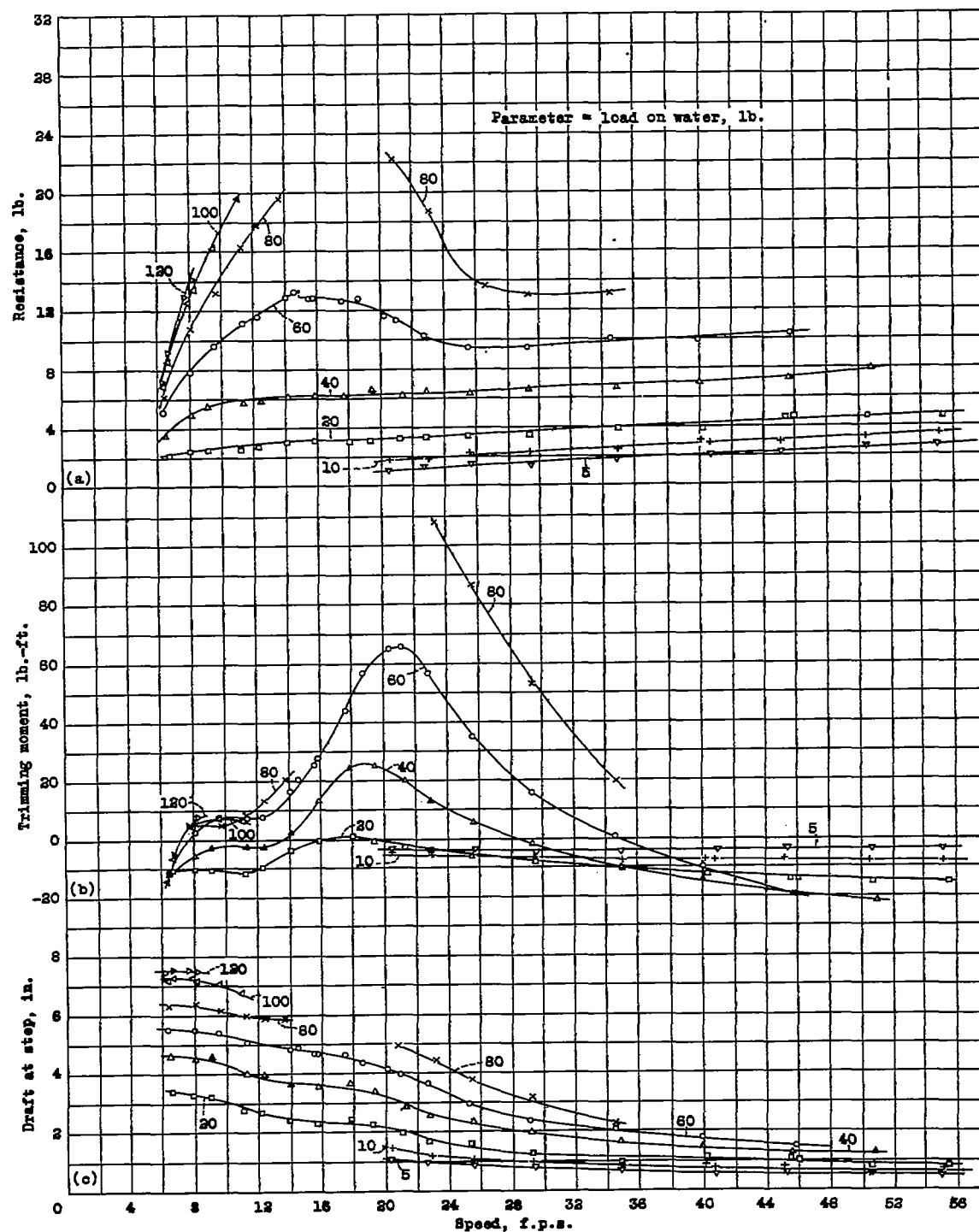
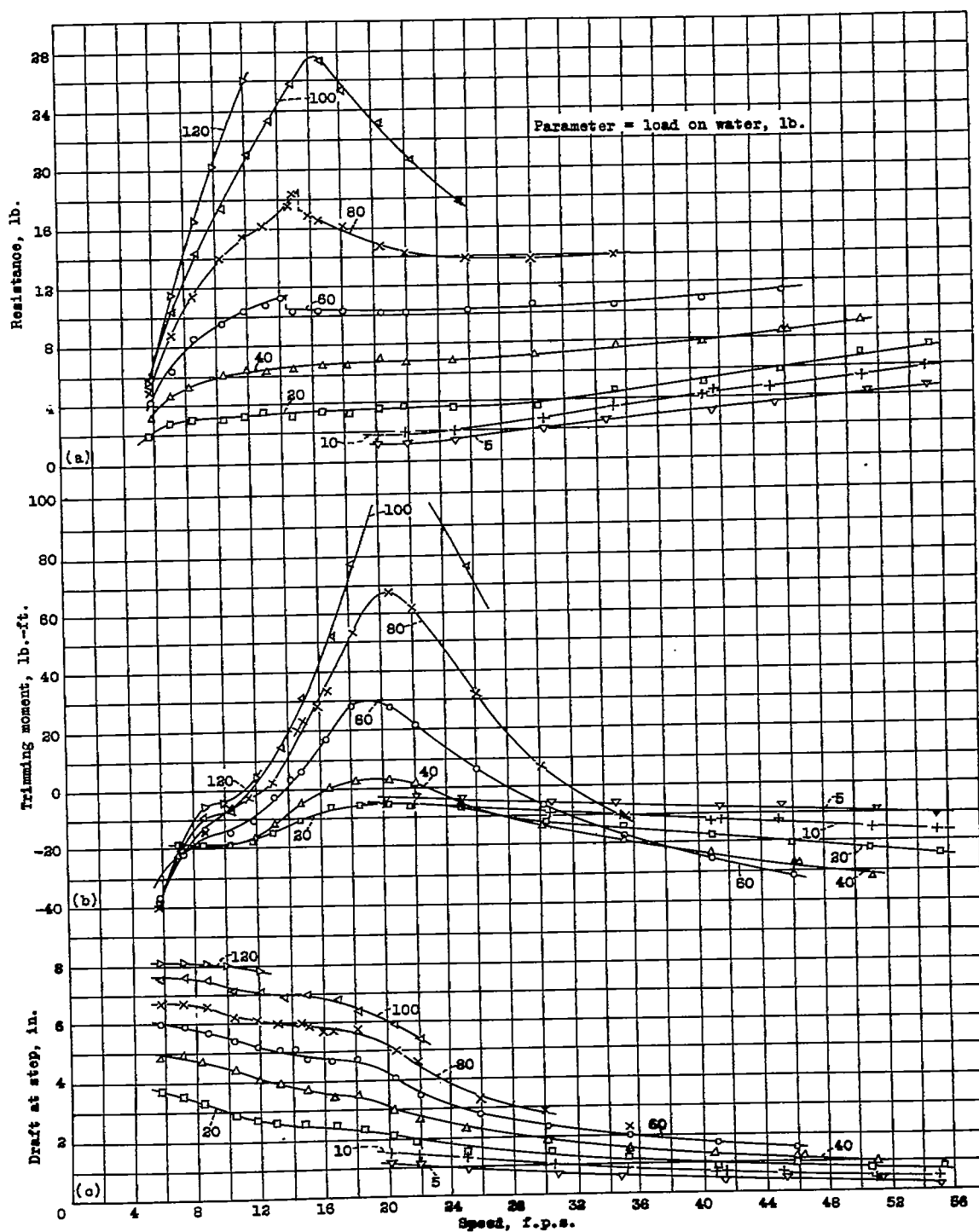


Figure 1.- Lines of N.A.O.A. model 35 series.

Figure 2.- Model 35. Resistance, trimming moment, and draft. $\tau = 3^\circ$.

Figure 3.- Model 35. Resistance, trimming moment, and draft. $\tau = 5^\circ$.


Figure 4.- Model 35. Resistance, trimming moment, and draft. $\tau = 70^\circ$.

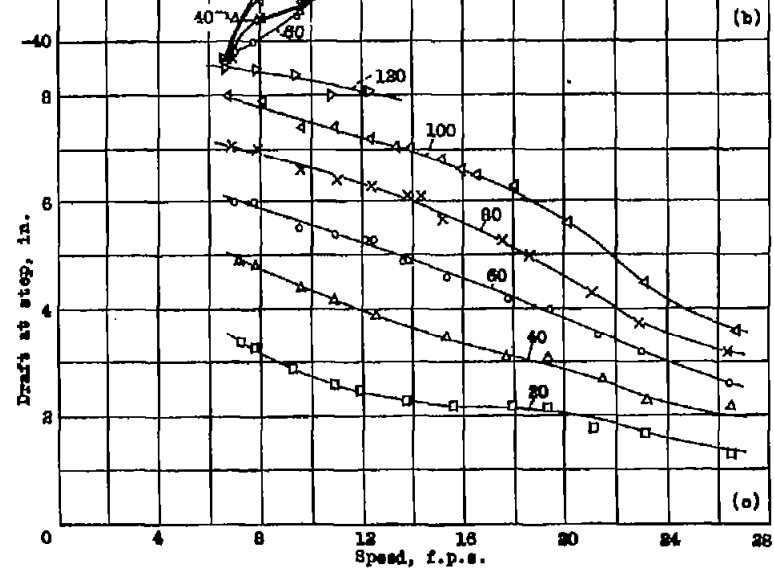
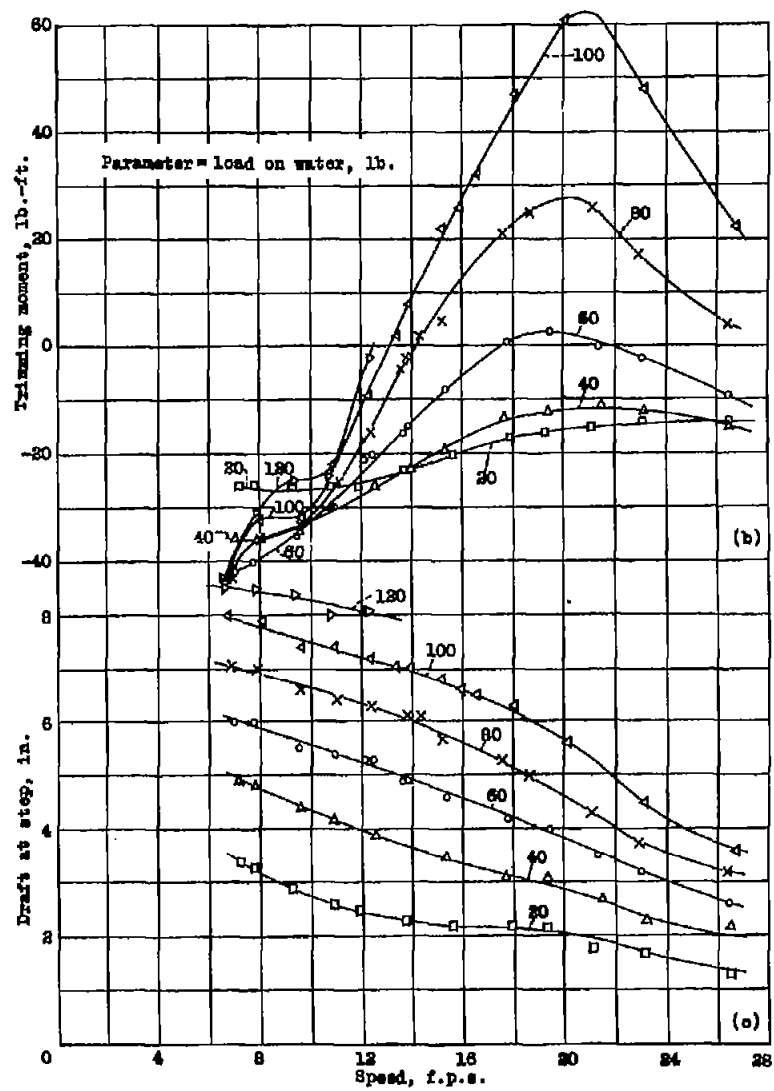
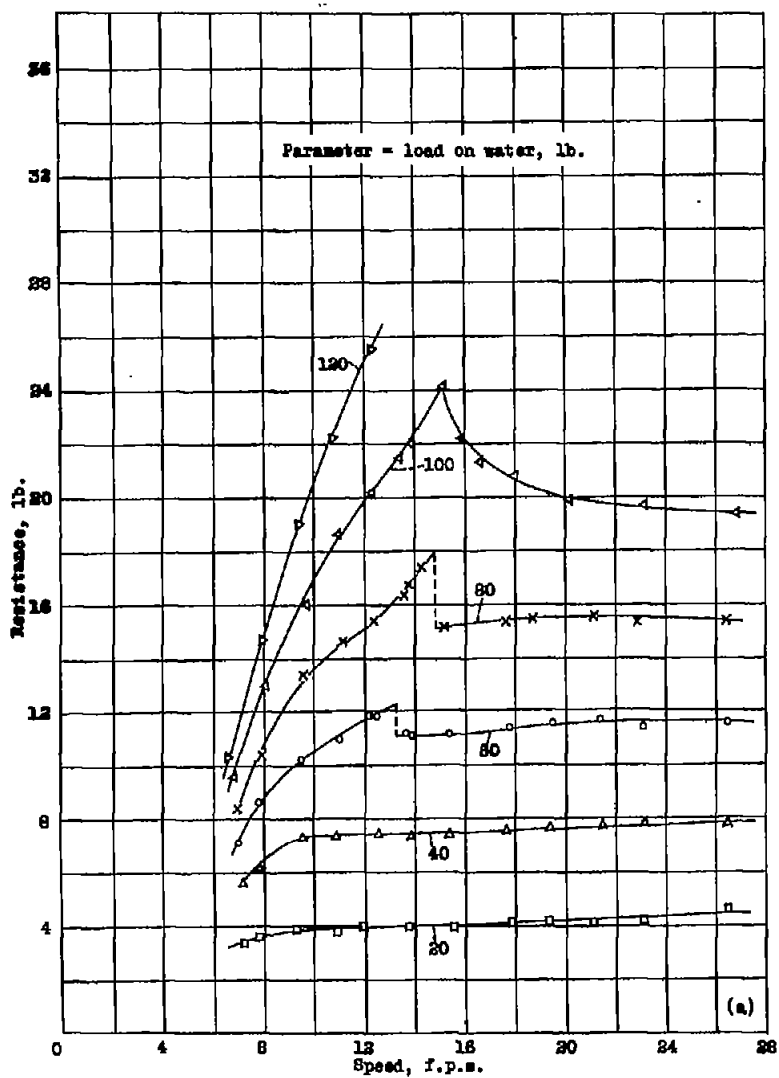


Figure 5.- Model 35. Resistance, trimming moment, and draft. $T = 90^\circ$.

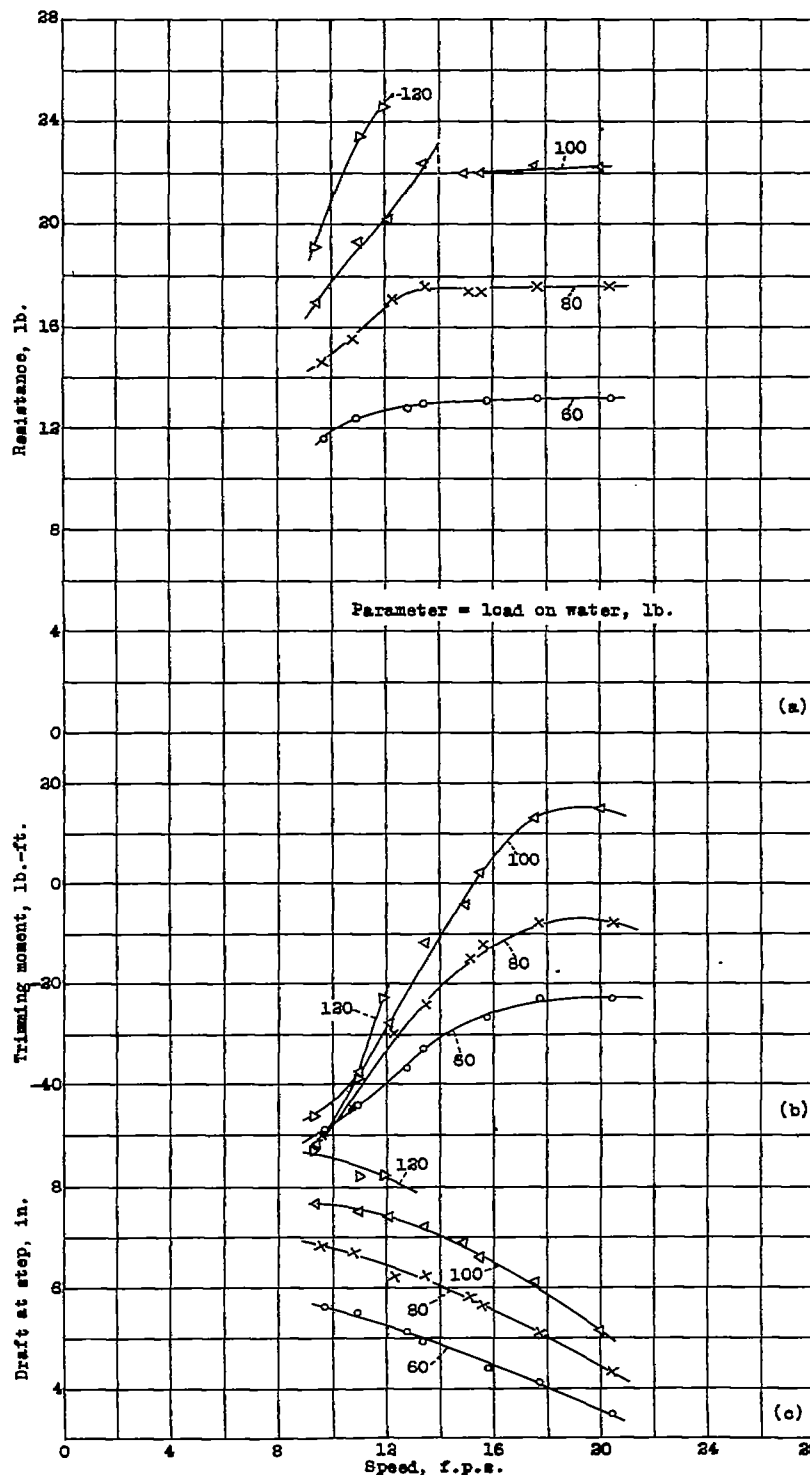


Figure 6.- Model 35. Resistance, trimming moment, and draft. $\tau = 11^\circ$.

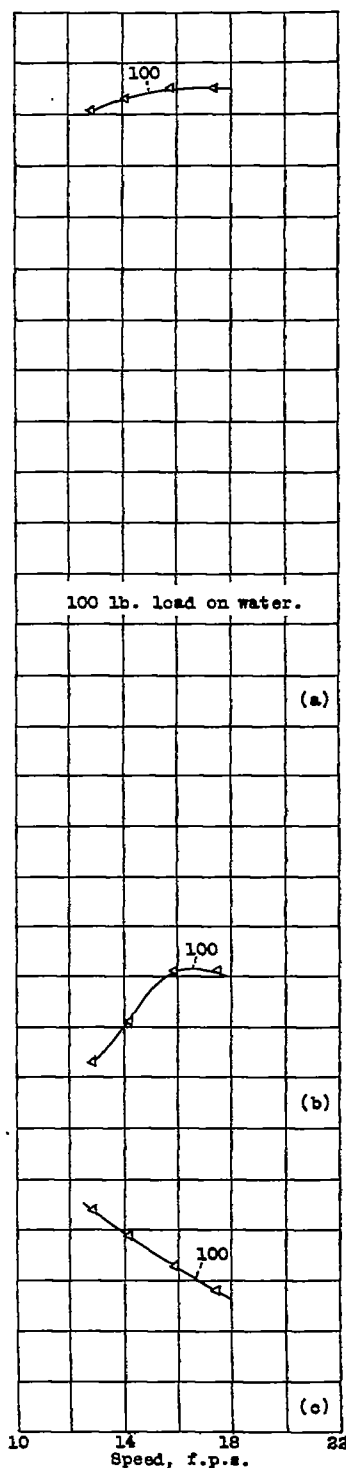


Figure 7.- Model 35. Resistance, trimming moment, and draft. $\tau = 13^\circ$.

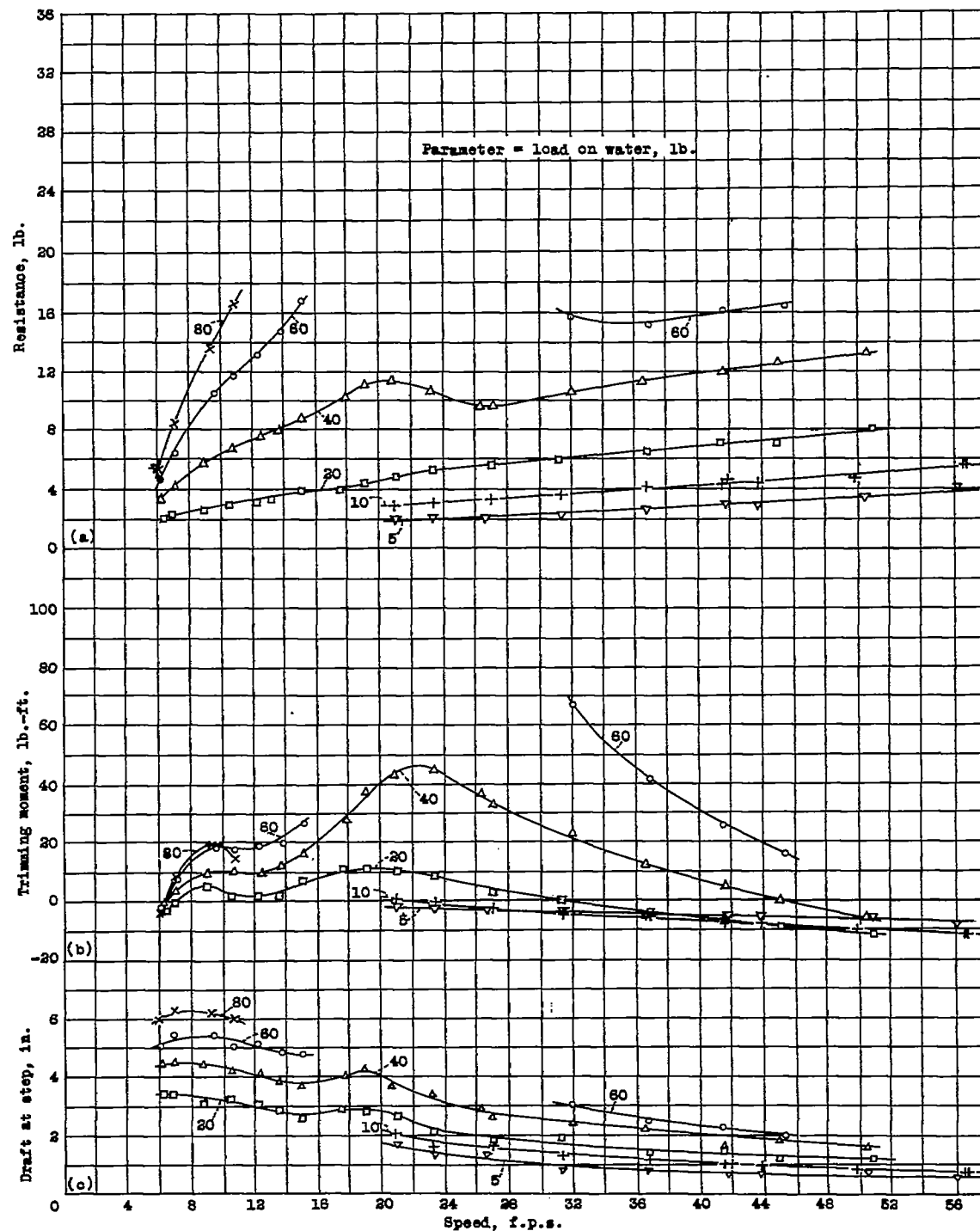
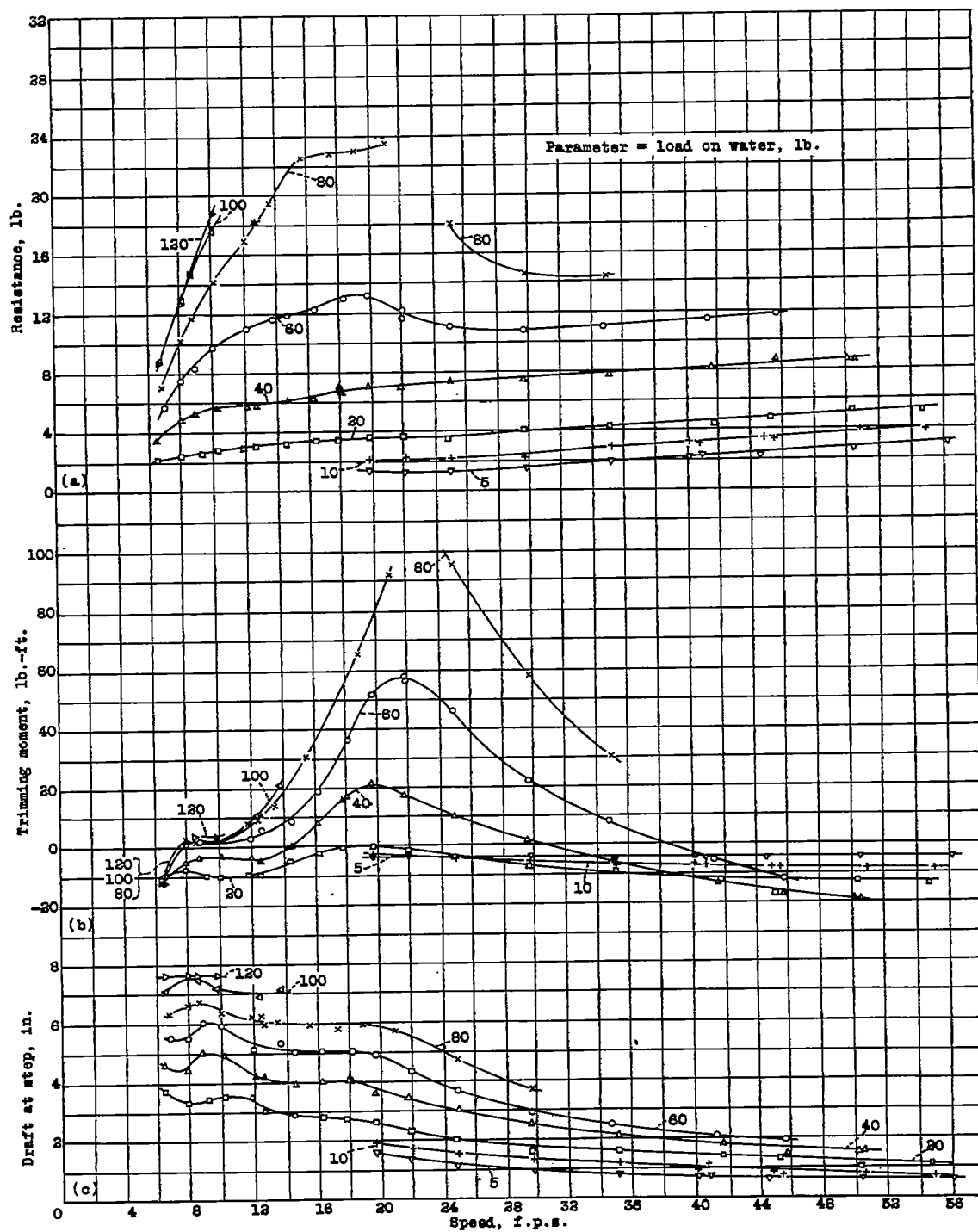


Figure 8.- Model 35-A. Resistance, trimming moment, and draft. $\tau = 30^\circ$.

Figure 9.- Model 35-A. Resistance, trimming moment, and draft. $\tau = 5^\circ$.

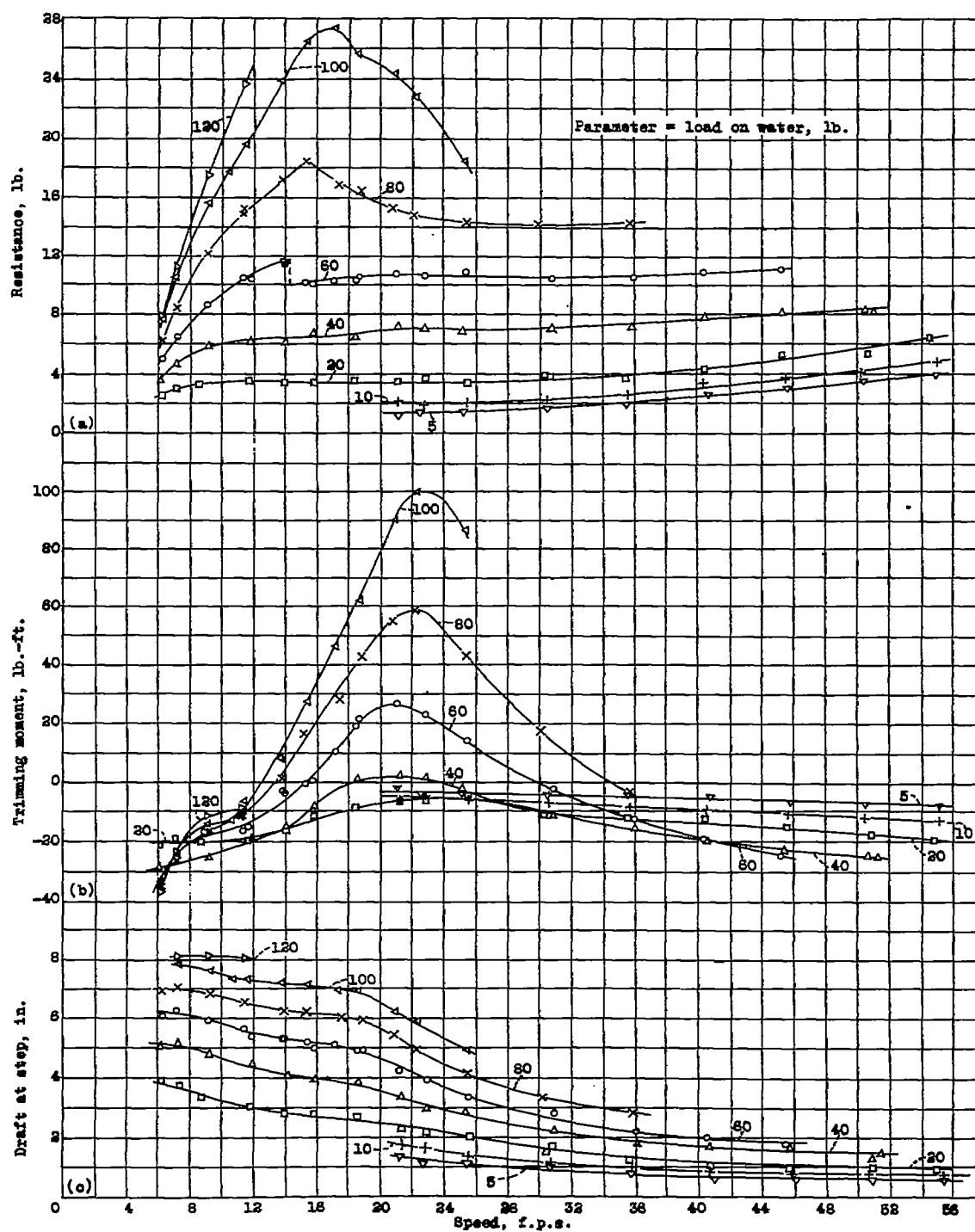
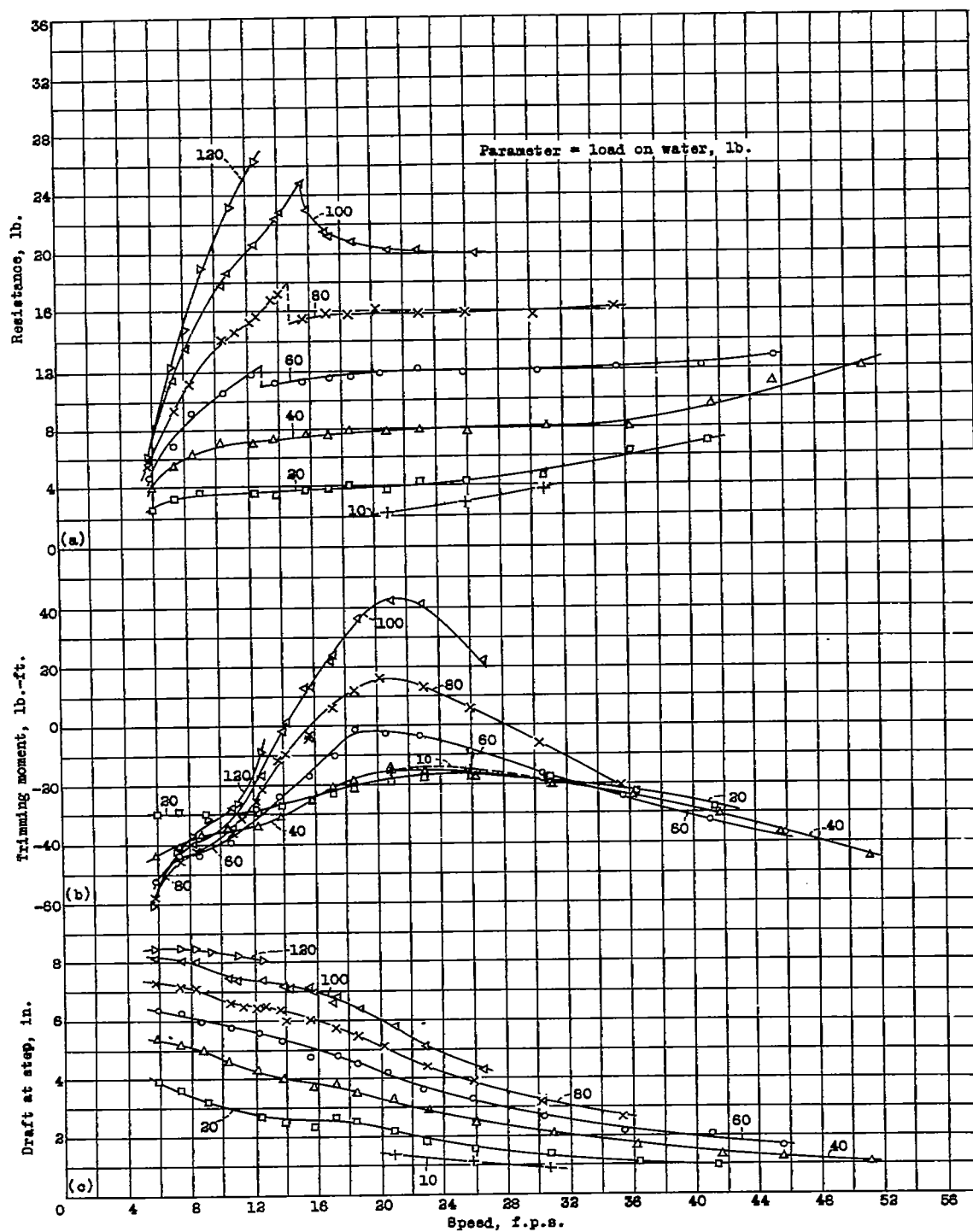


Figure 10.- Model 35-A. Resistance, trimming moment, and draft. $\tau = 7^\circ$.

Figure 11.- Model 35-A. Resistance, trimming moment, and draft. $\tau = 90^\circ$.

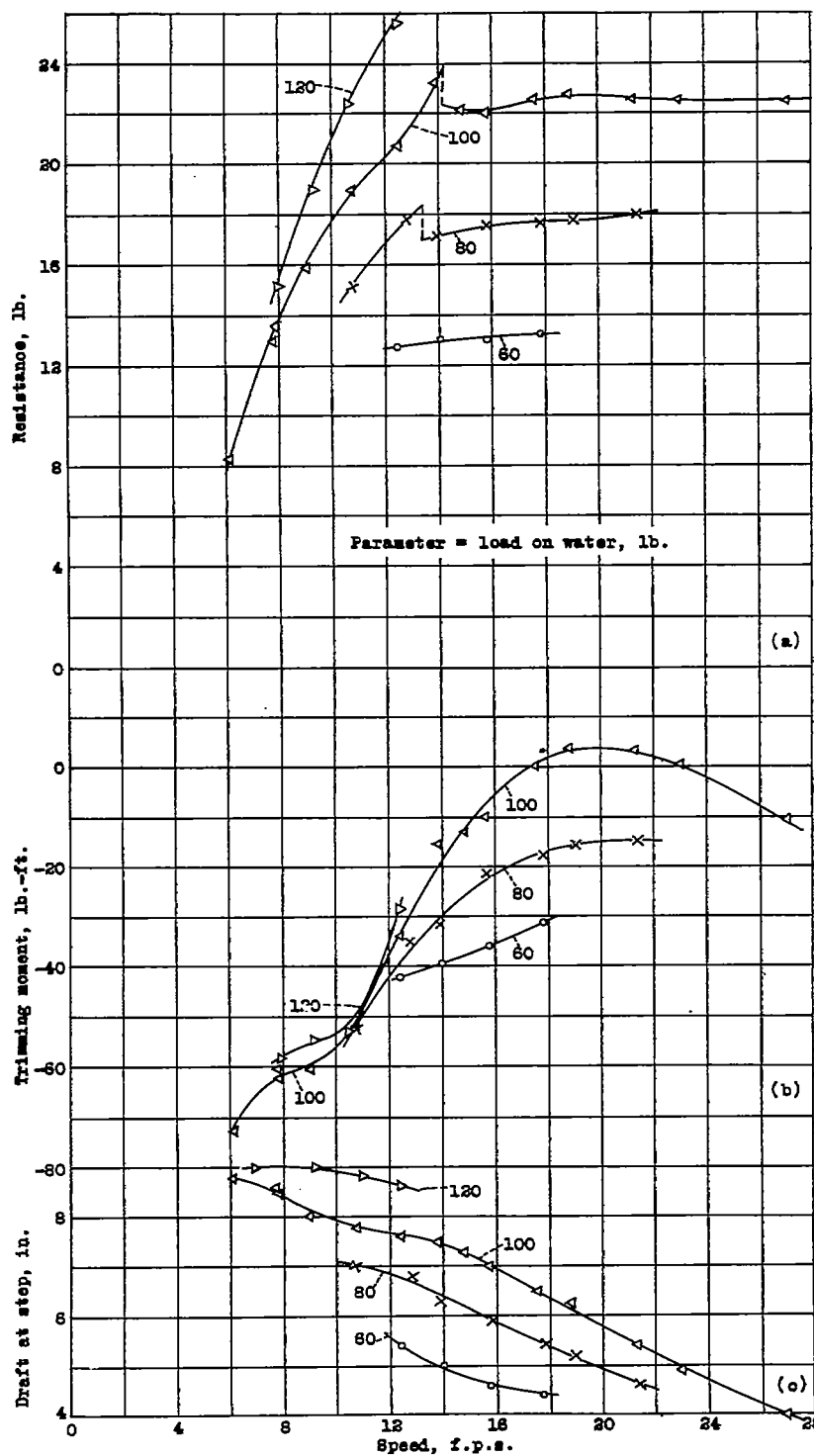


Figure 12.- Model 35-A. Resistance, trimming moment, and draft. $\tau = 110^\circ$.

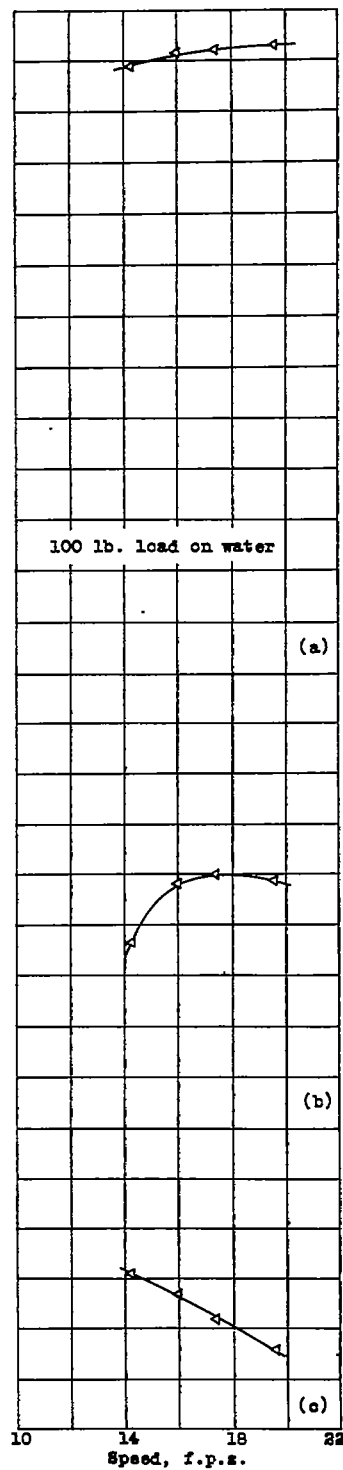
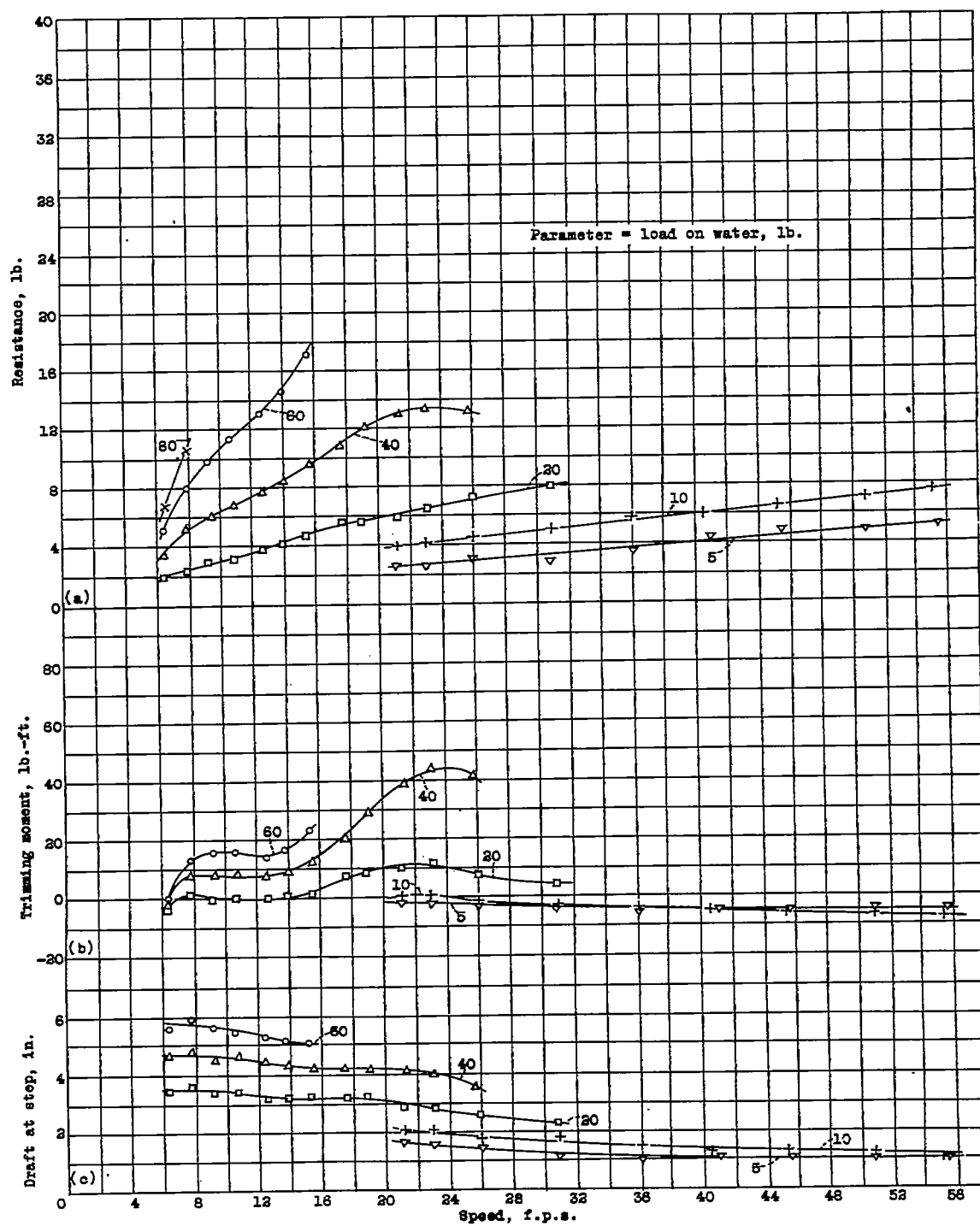
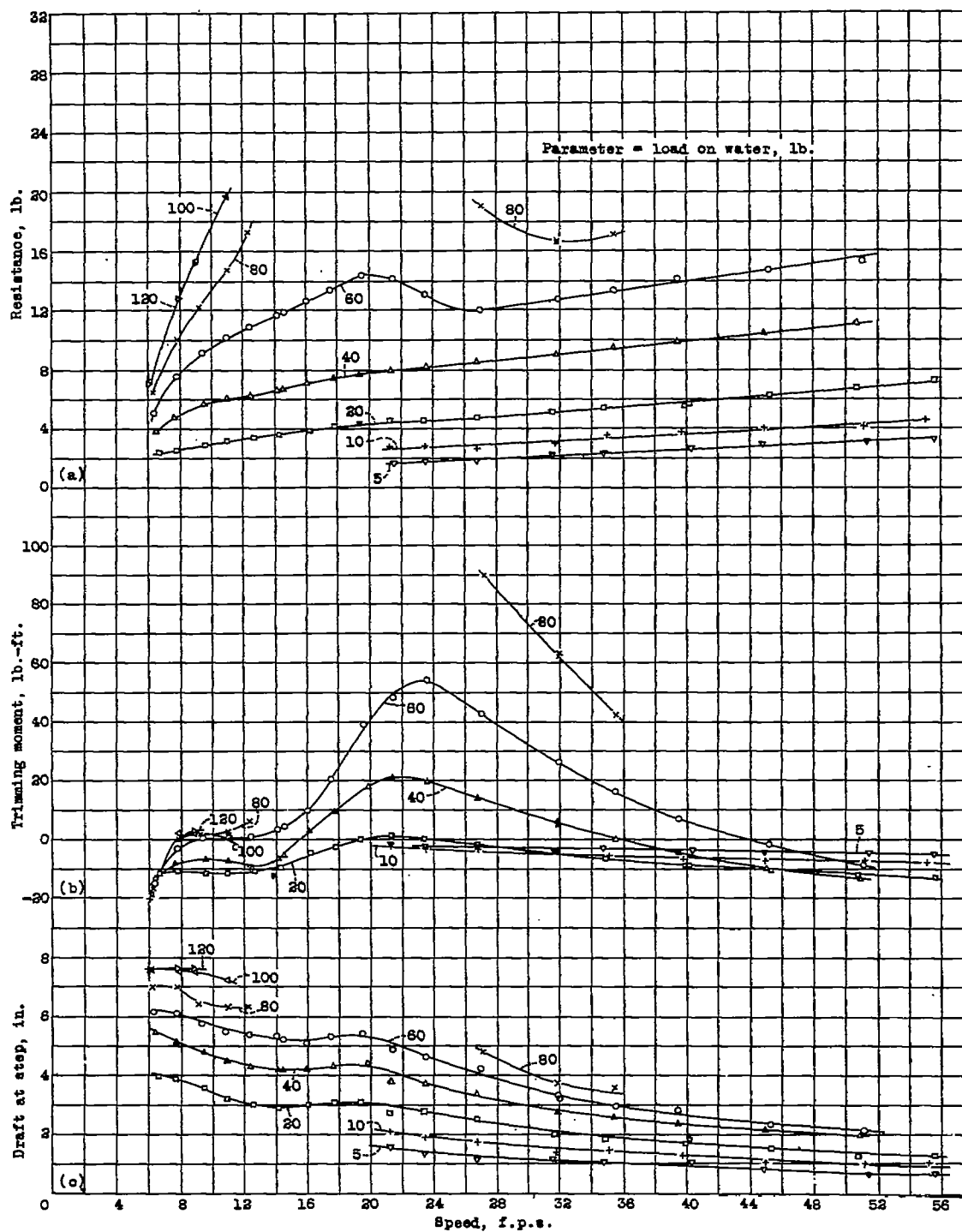


Figure 13.- Model 35-A. Resistance, trimming moment, and draft. $\tau = 130^\circ$.

Figure 14.- Model 35-B. Resistance, trimming moment, and draft. $\tau = 3^\circ$.


Figure 15.- Model 35-B. Resistance, trimming moment, and draft. $\tau = 5^\circ$.

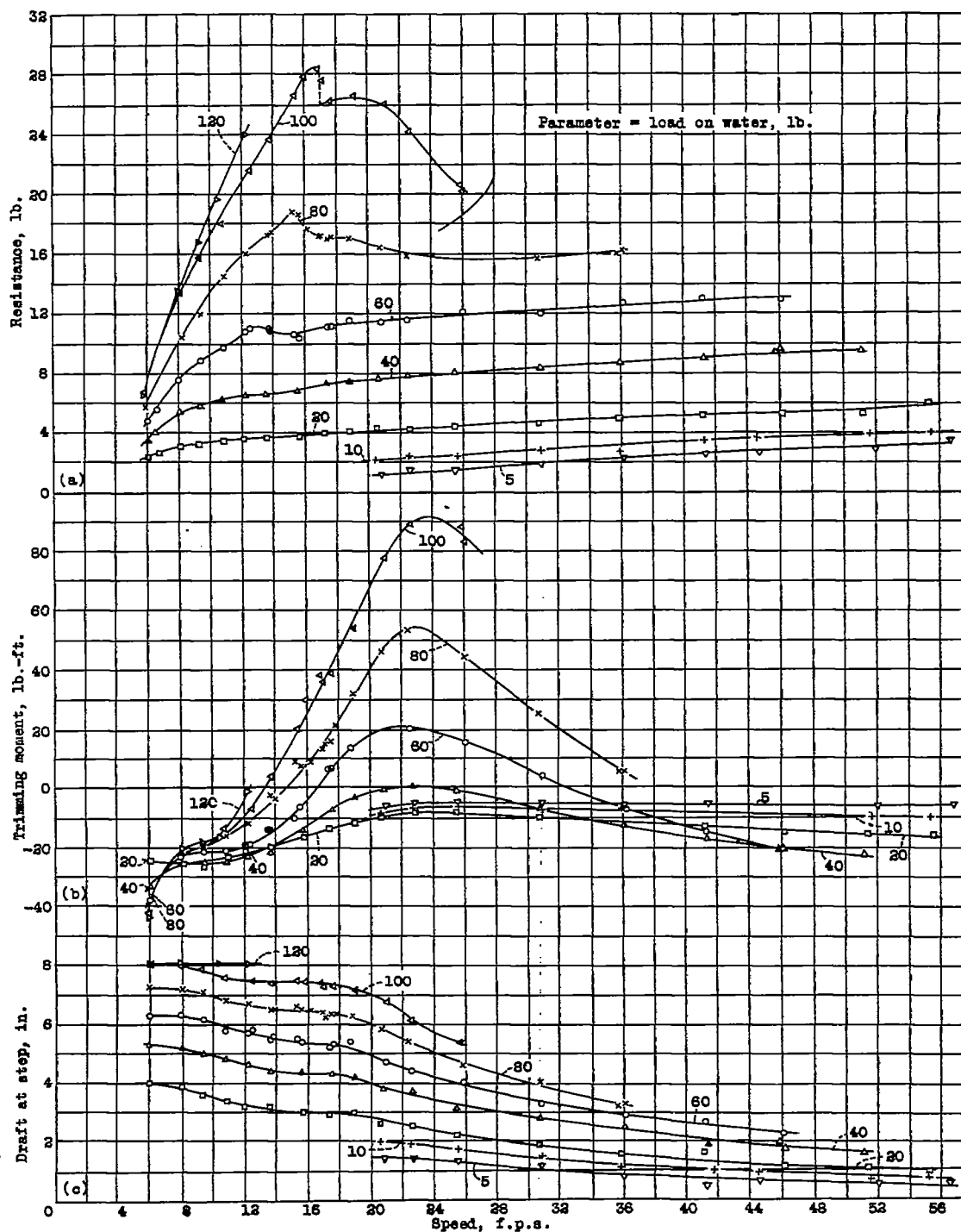
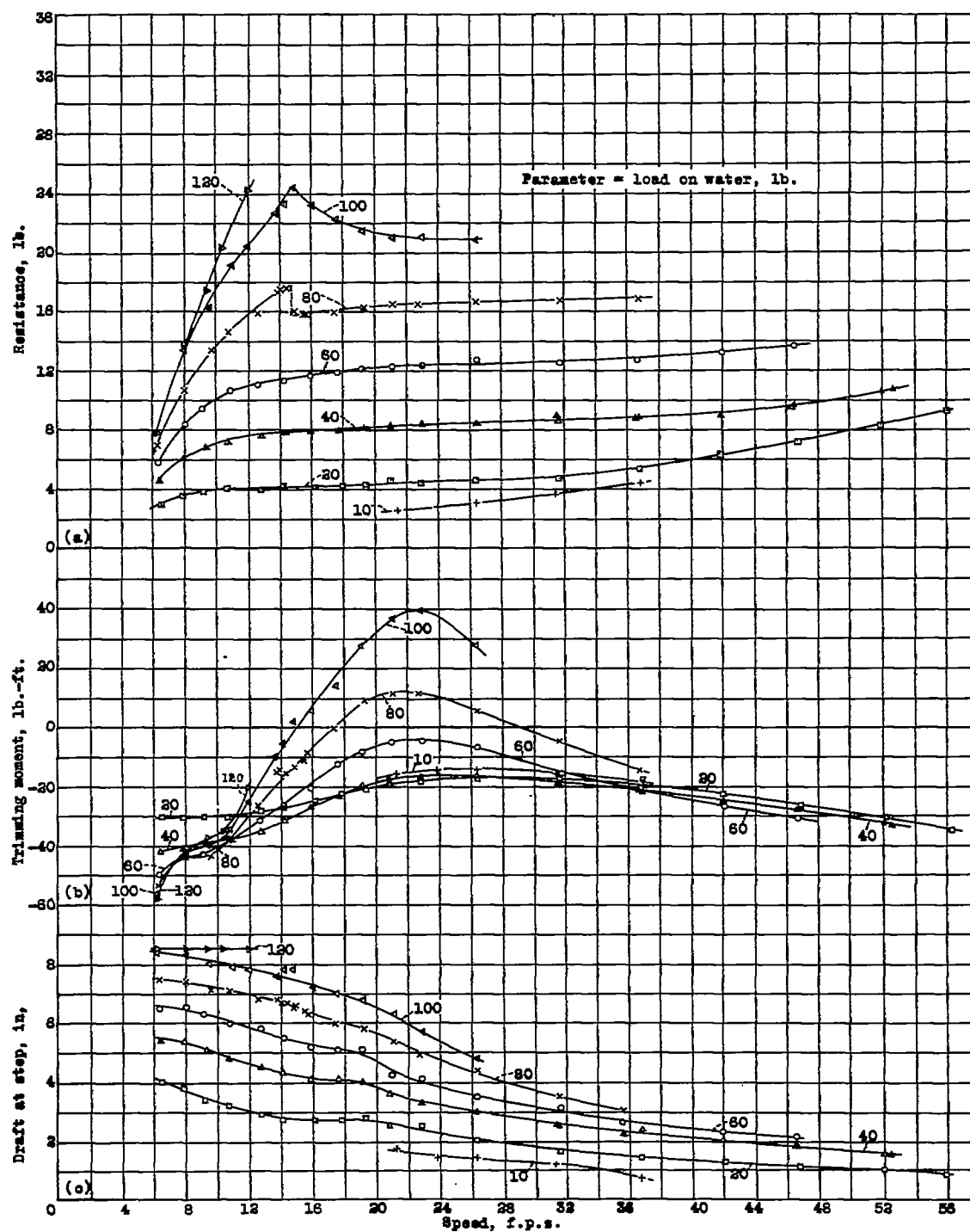


Figure 16.- Model 35-B. Resistance, trimming moment, and draft. $\gamma = 7^\circ$.

Figure 17.- Model 35-B. Resistance, trimming moment, and draft. $\tau = 9^\circ$.

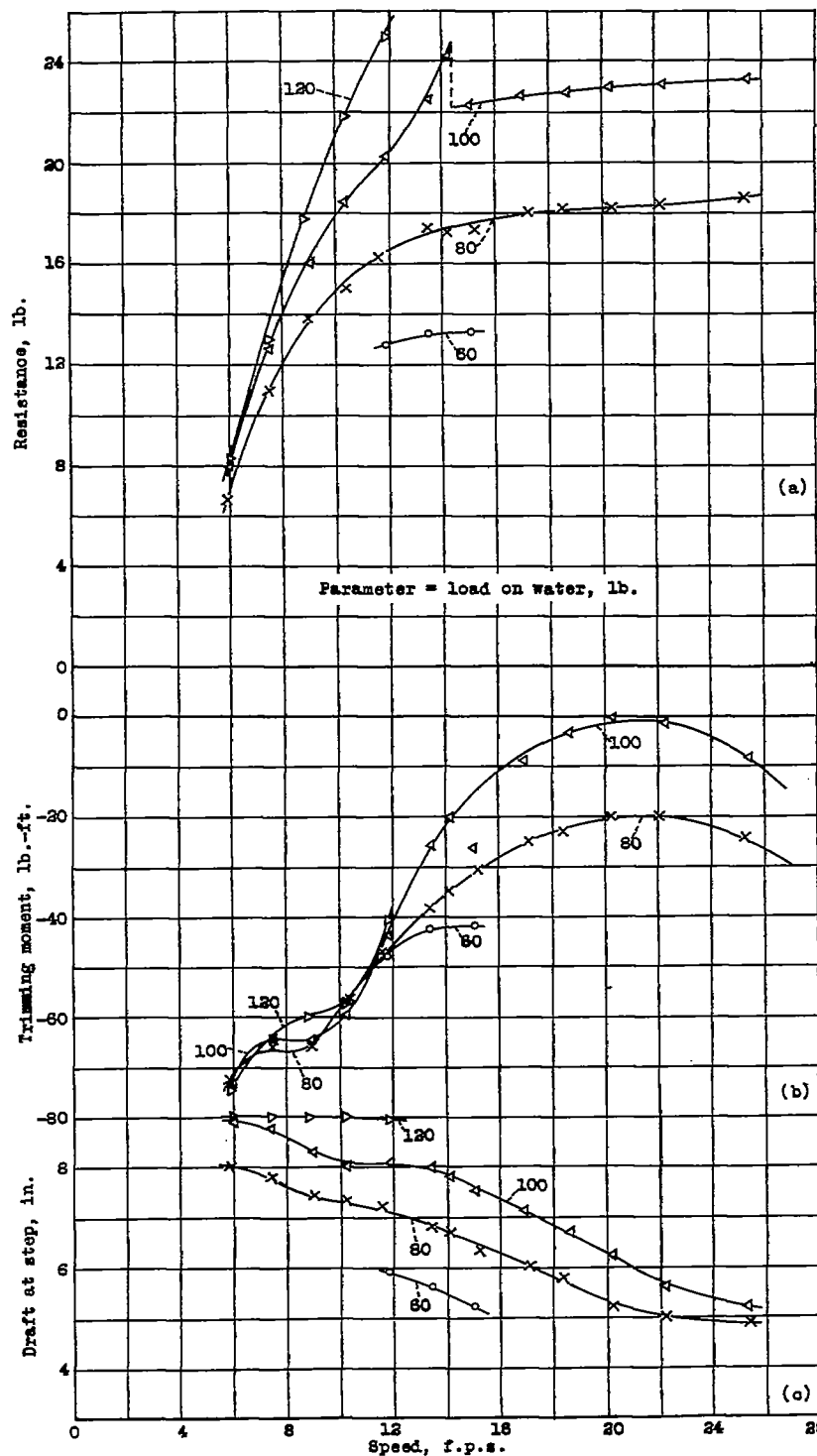


Figure 18.- Model 35.- Resistance, trimming moment, and draft. $\tau = 11^\circ$

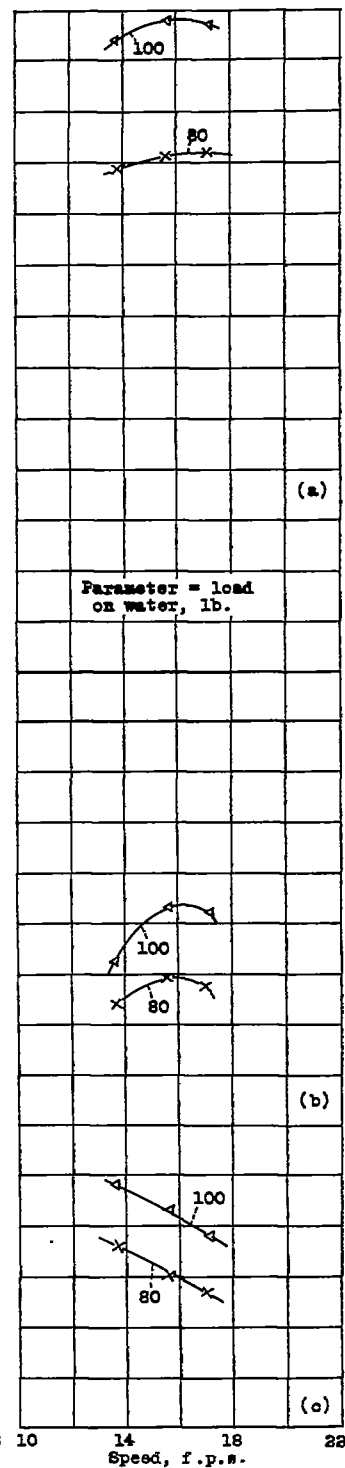


Figure 19.- Model 35-B.- Resistance, trimming moment, and draft. $\tau = 13^\circ$

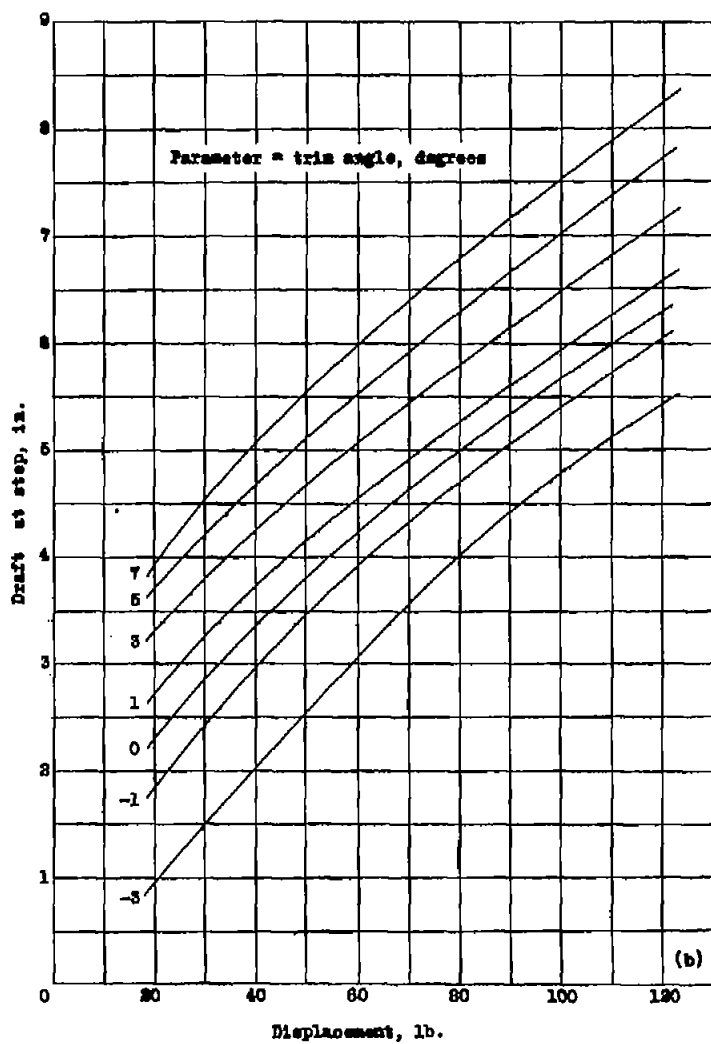
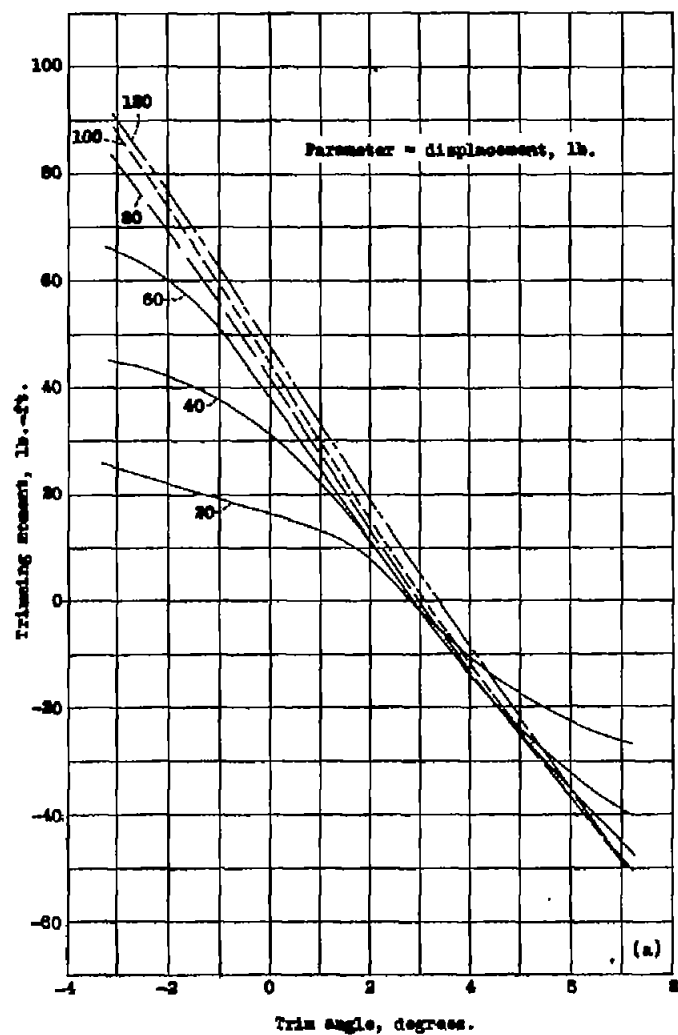


Figure 20a,b.- Model 35-A. Static trimming moments and drafts.

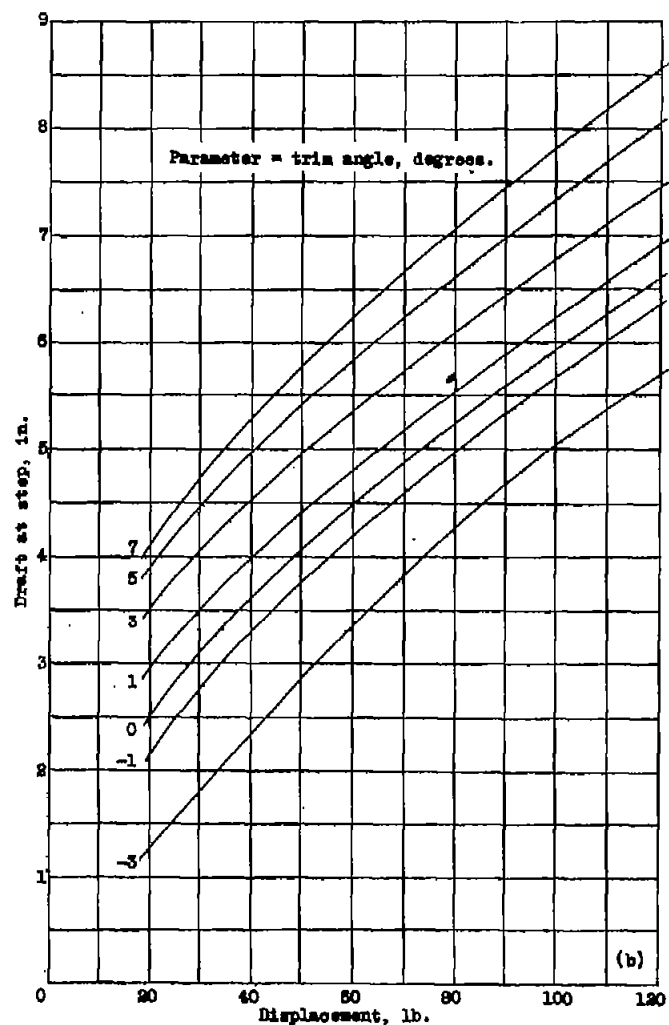
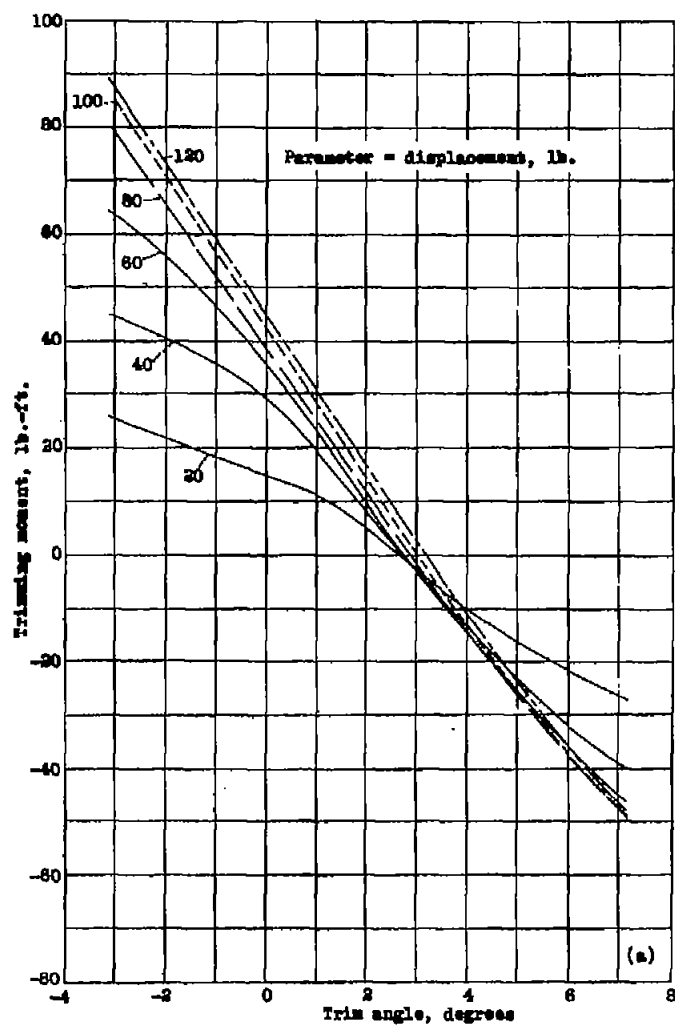


Figure 21 a,b.- Model 36-B. Static trimming moments and drafts.

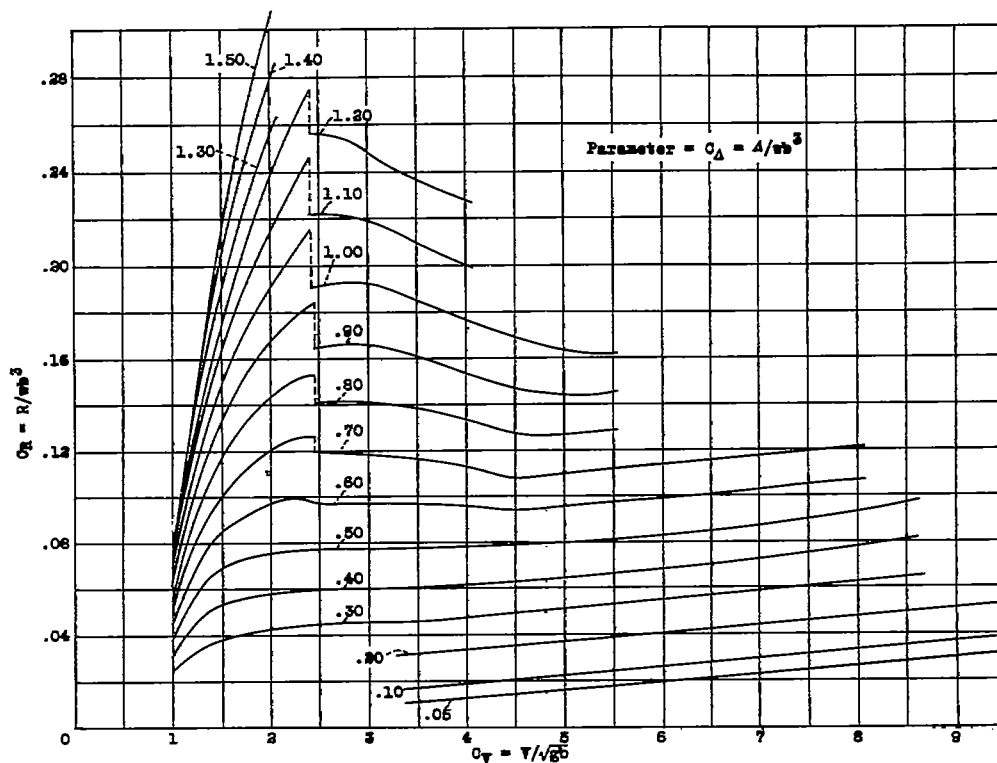


Figure 22.- Model 35. Variation of C_R at best trim angle with C_Y .

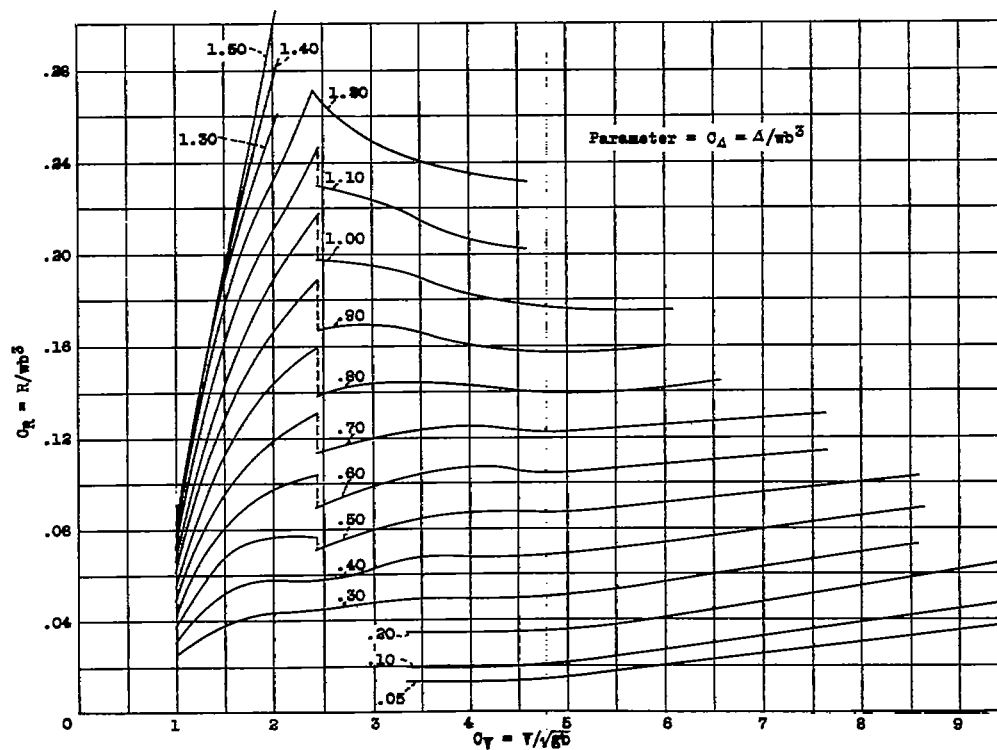
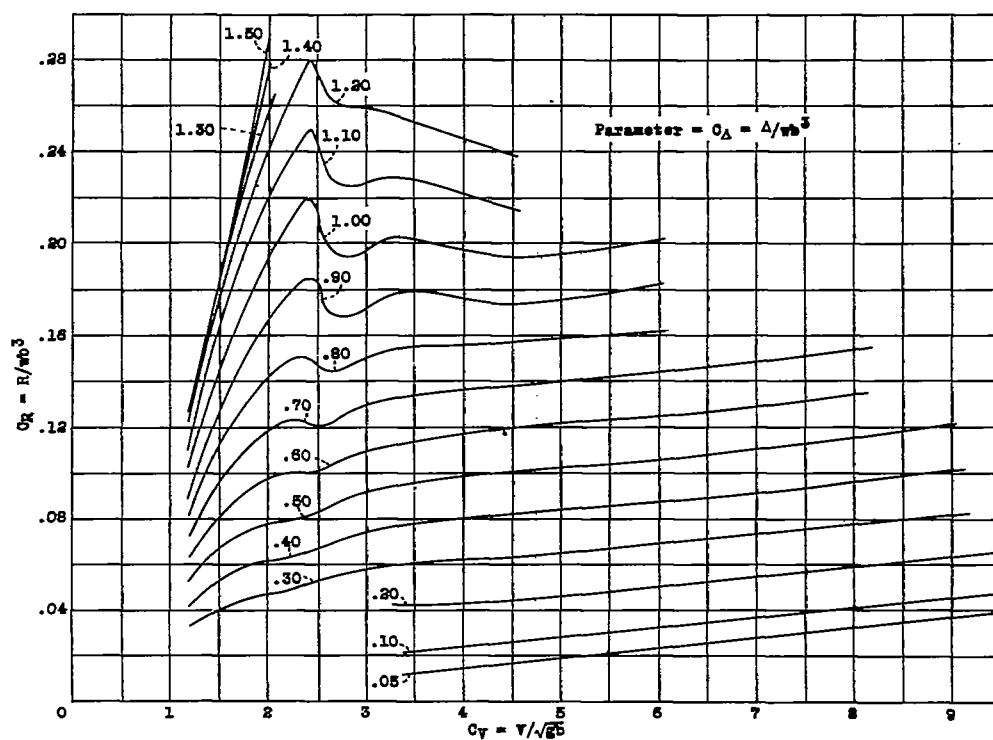
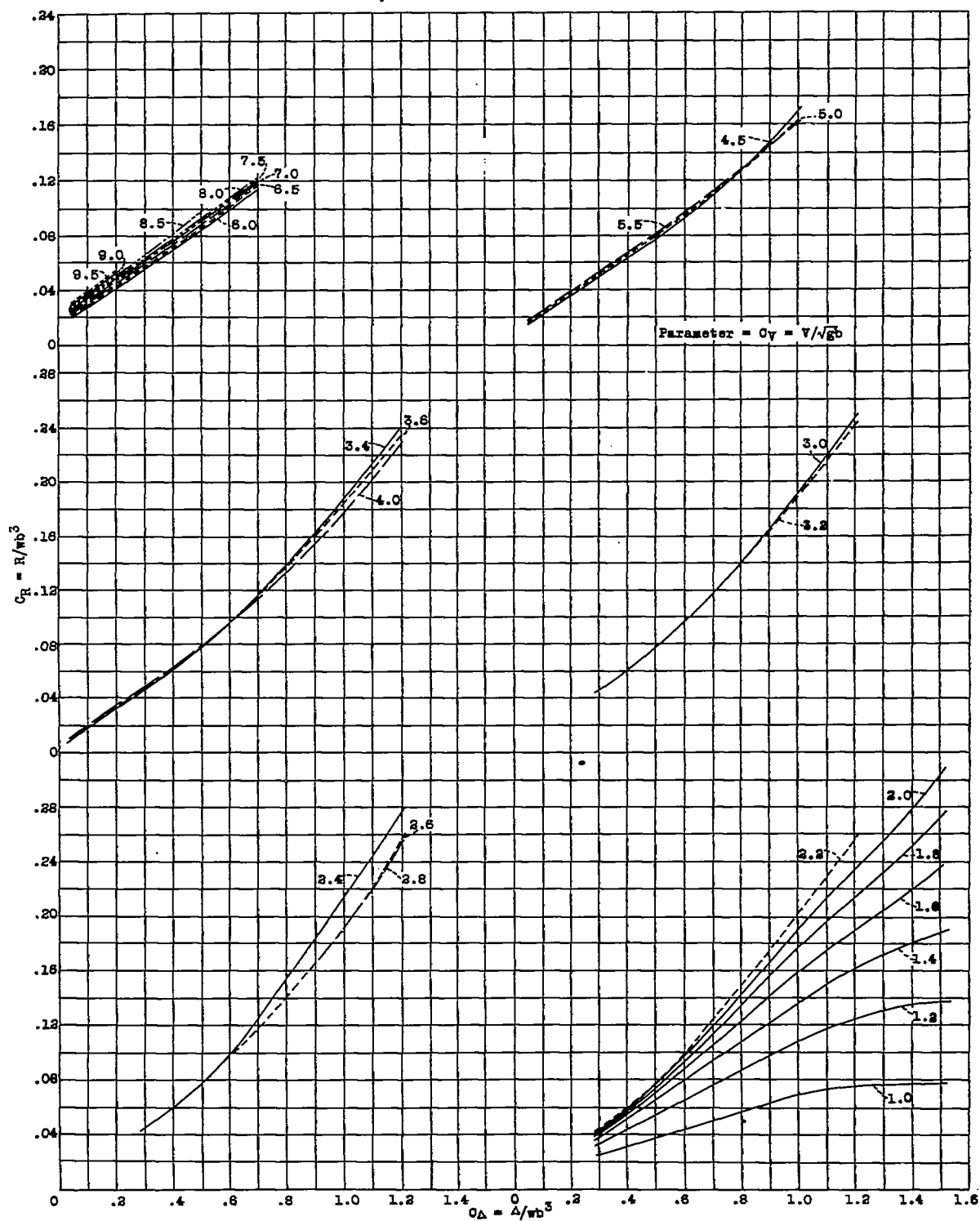


Figure 23.- Model 35-A. Variation of C_R at best trim angle with C_Y .

Figure 24.- Model 35-B. Variation of C_R at best trim angle with C_Y .


Figure 25.- Model 35.- Variation of C_R at best trix angle with C_{Δ} .

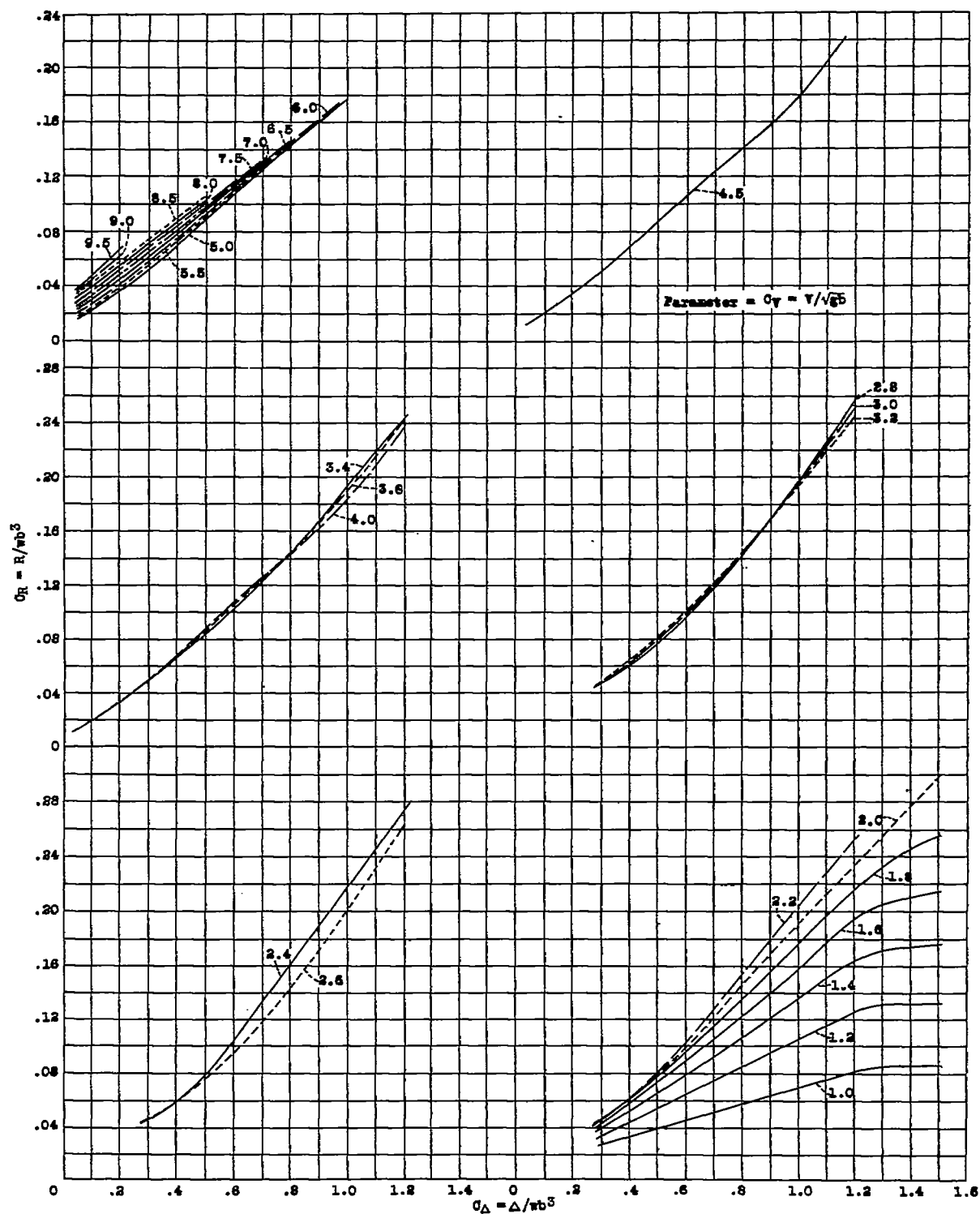
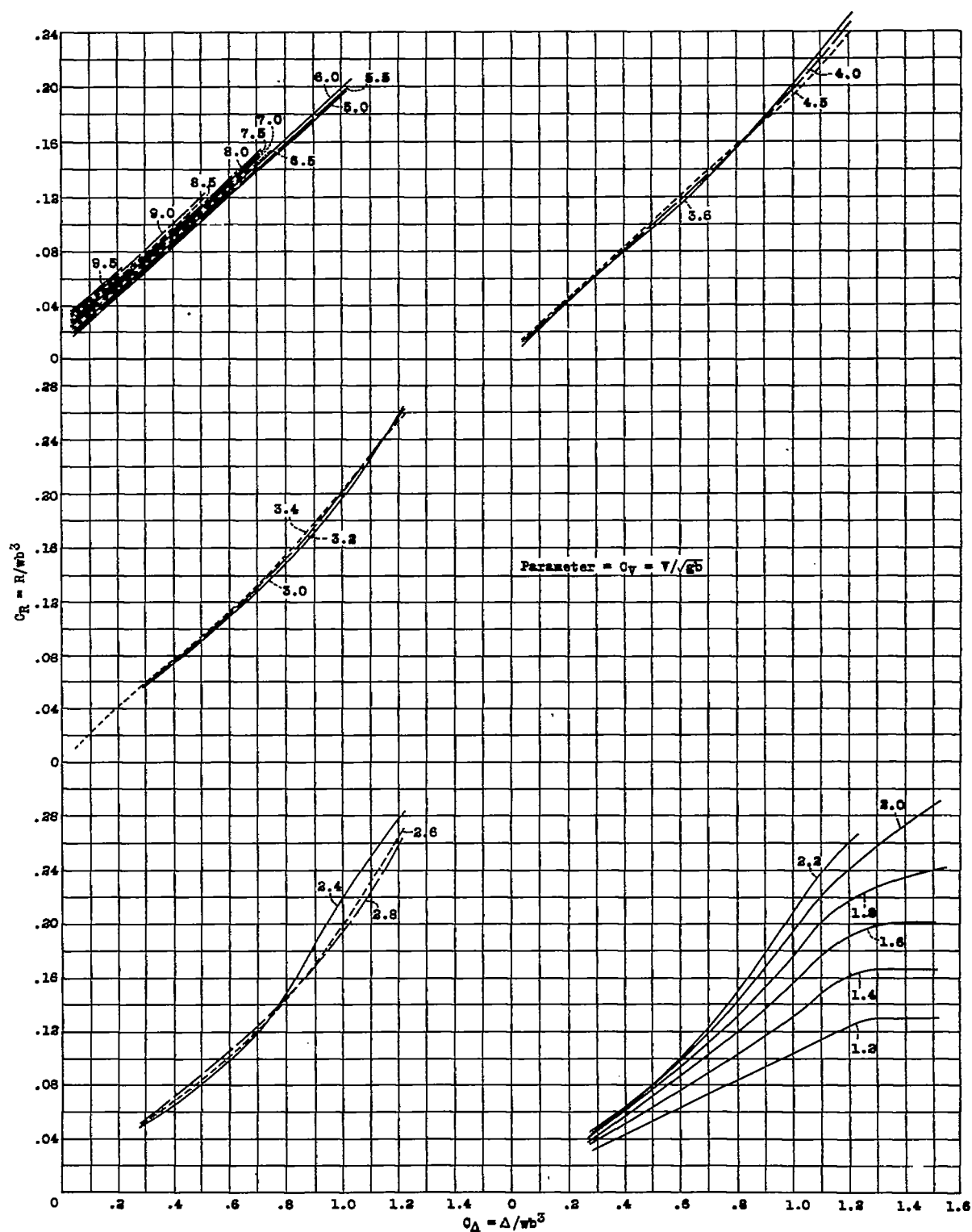


Figure 28.- Model 35-A. Variation of C_R at best trim angle with $C_{D\Delta}$.


Figure 27.- Model 35-B. Variation of C_R at best trim angle with Q_A .

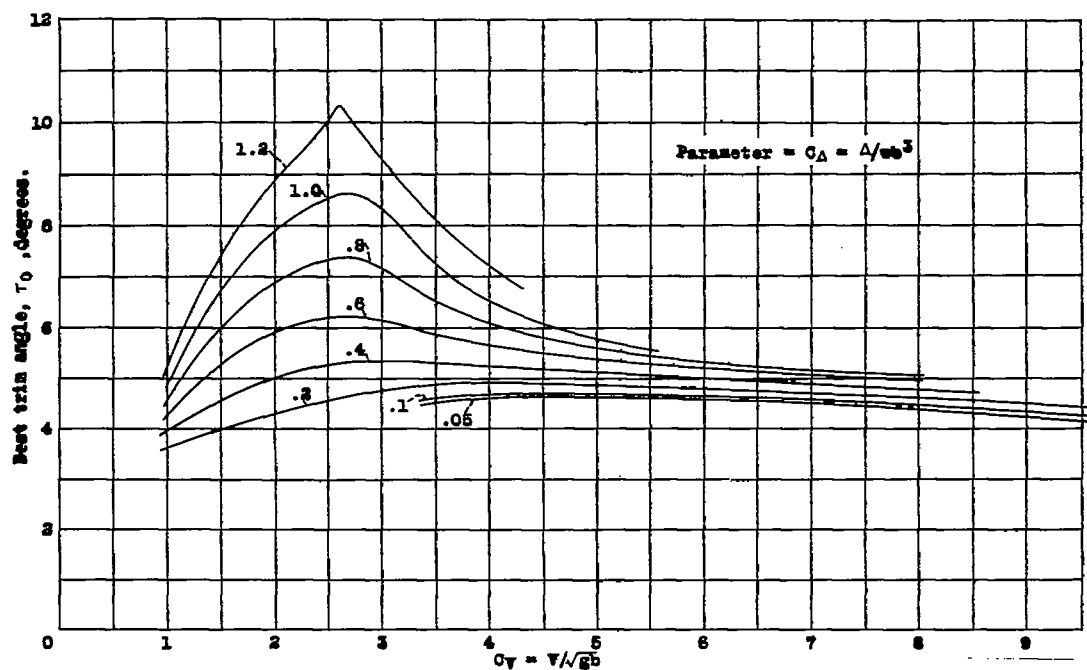


Figure 28.- Model 35. Variation of best trim angle with C_y .

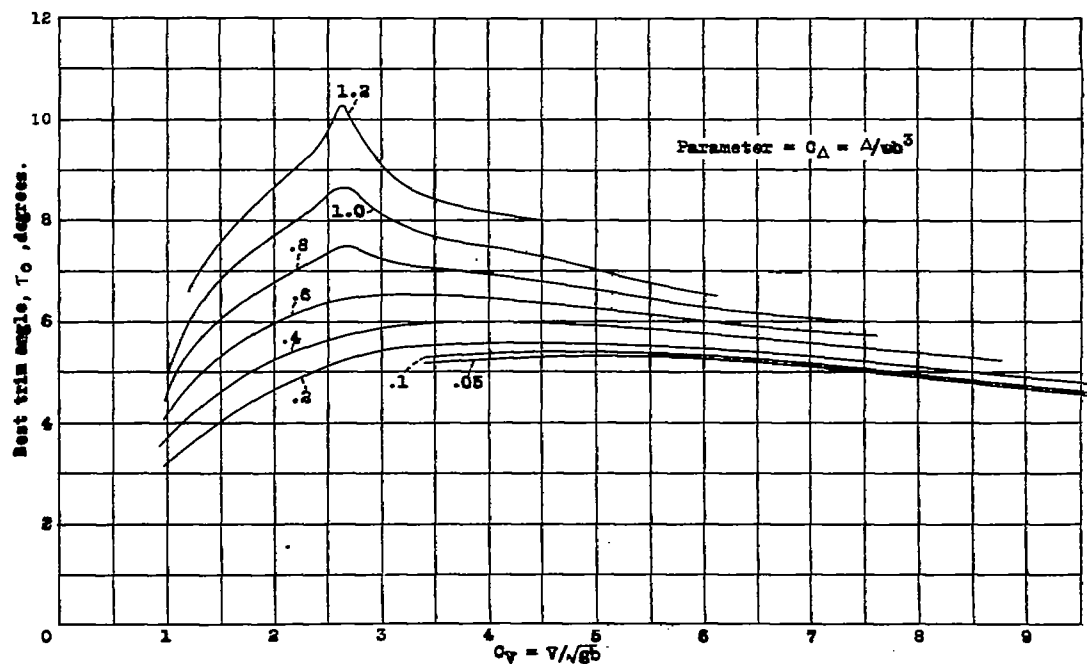


Figure 29.- Model 35-A. Variation of best trim angle with C_y .

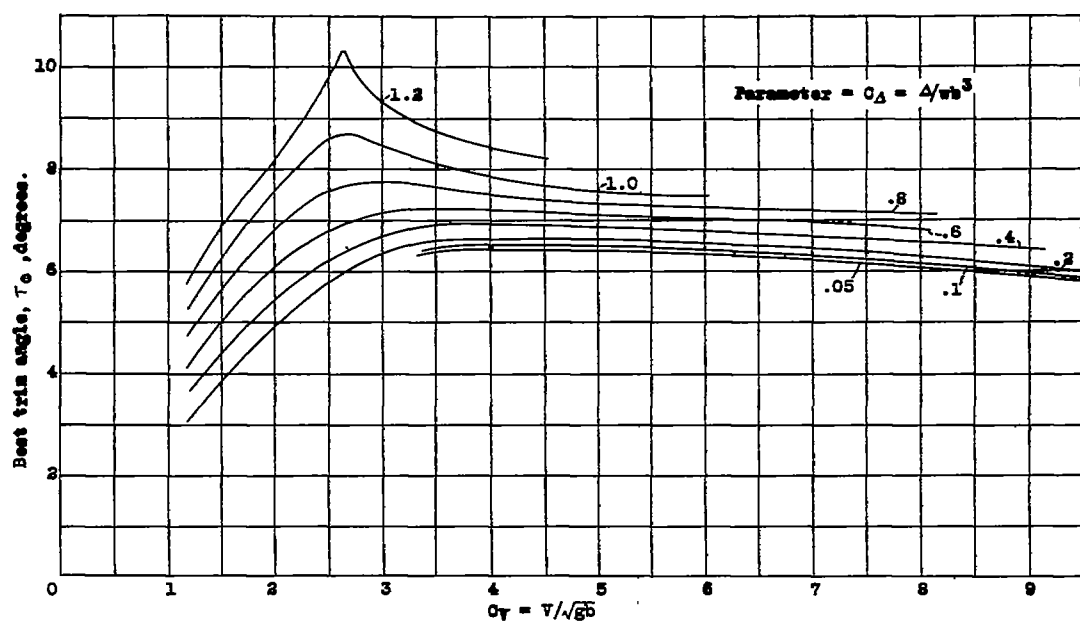


Figure 30.- Model 35-B. Variation of best trim angle with Cy .

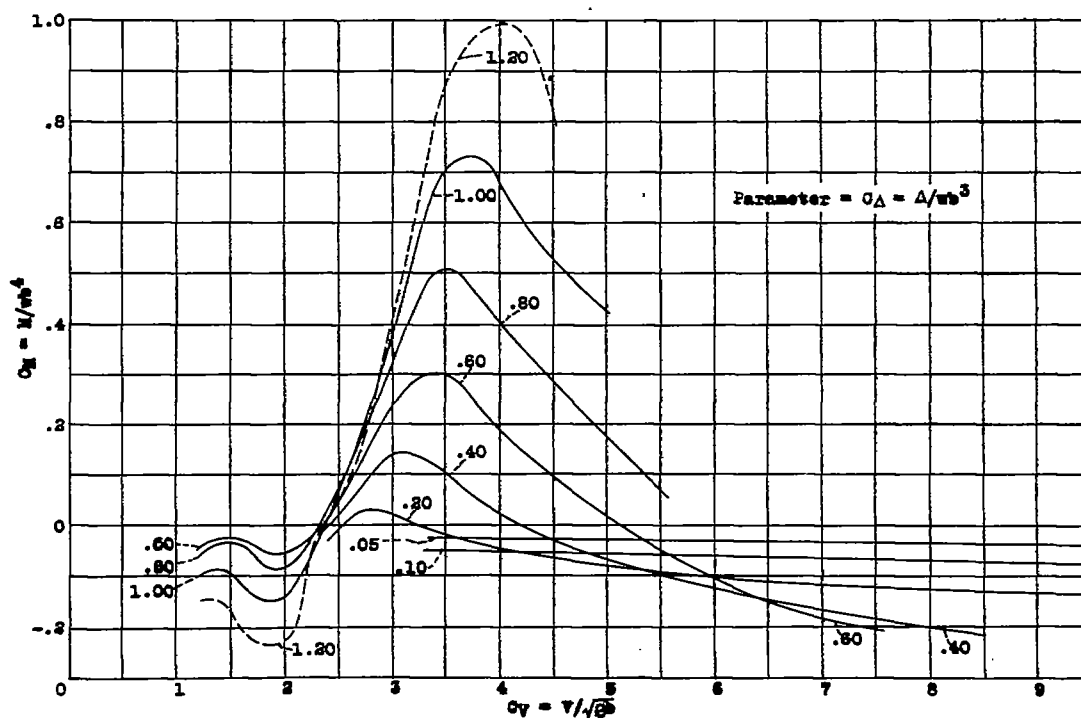


Figure 31.- Model 35. Variation of C_y at best trim angle with Cy .

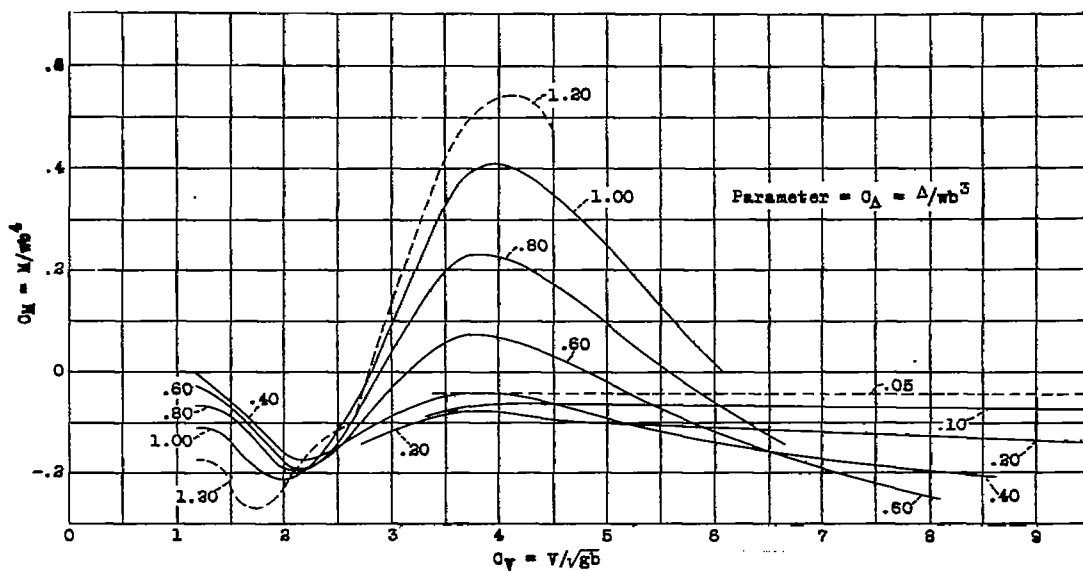


Figure 33.- Model 35-B. Variation of C_M at best trim angle with C_V .

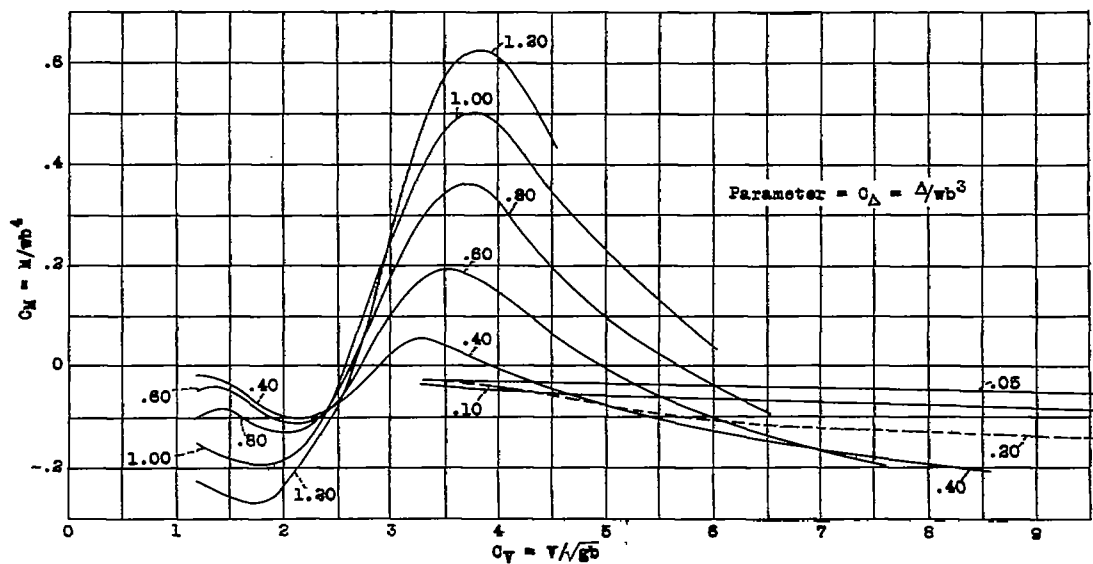


Figure 32.- Model 35-A. Variation of C_M at best trim angle with C_V .

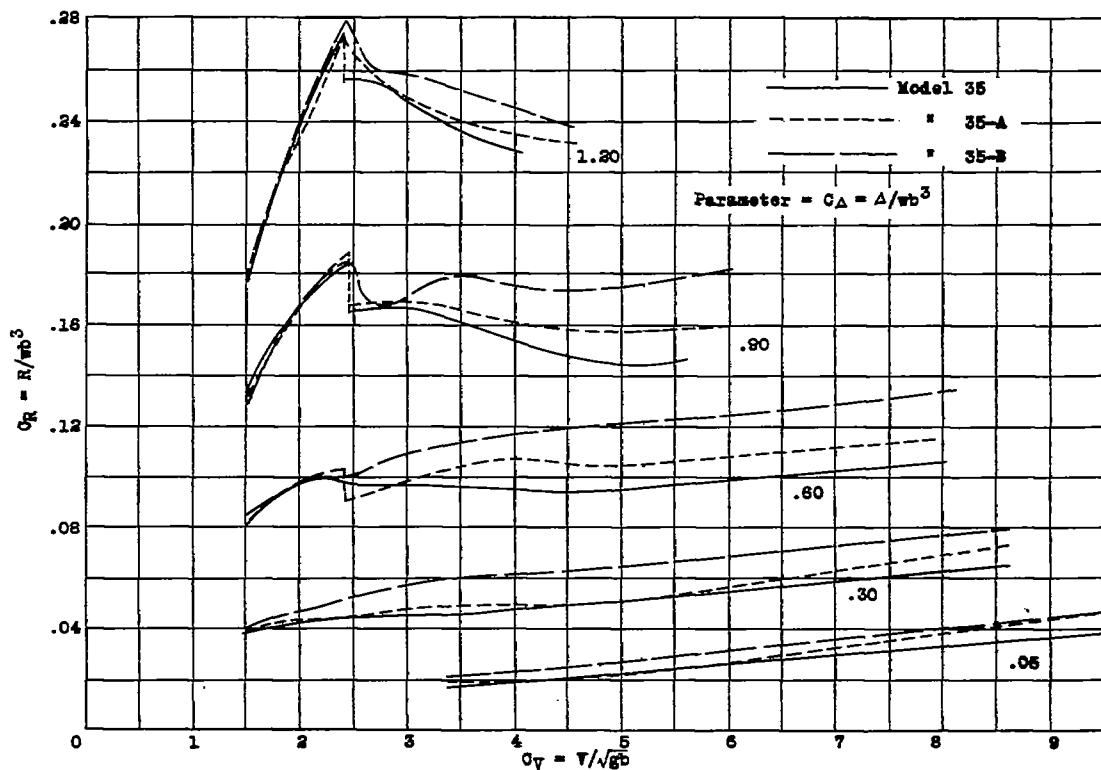


Figure 34.- Effect of angle of dead rise on C_R at best trim angle.

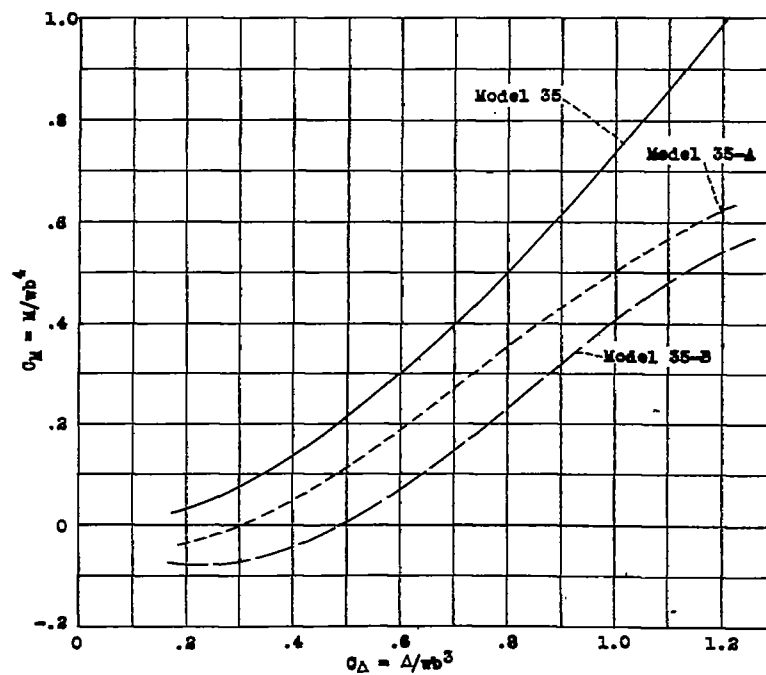


Figure 35.- Effect of angle of dead rise on maximum positive C_T at best trim angle.

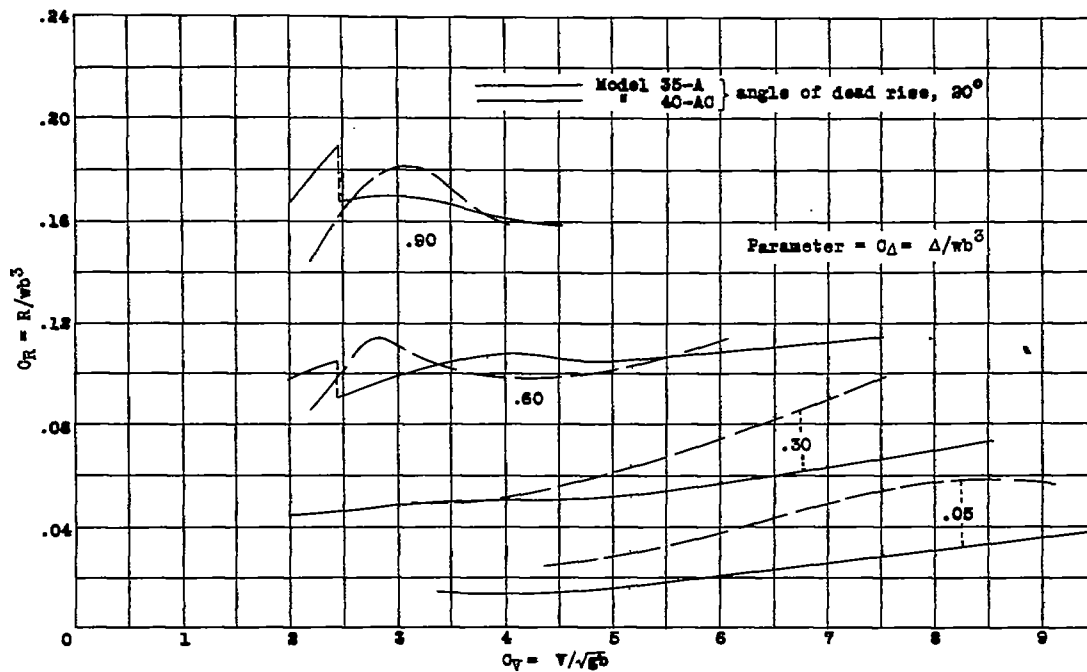


Figure 36.- Comparison of resistance of models 35-A and 40-A0.

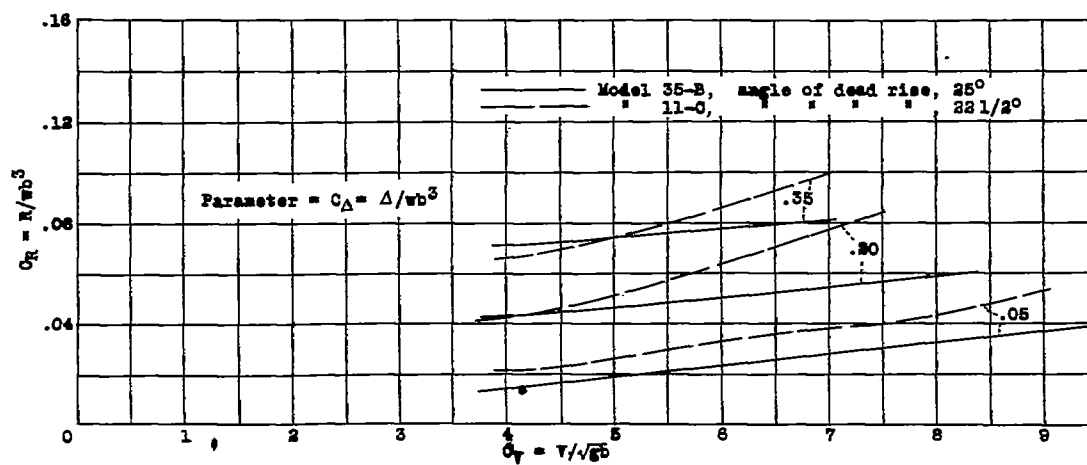


Figure 37.- Comparison of resistance of models 35-B and 11-C.